

T/M Lee

NUREG/CR-3046
PNL-4385
Vol. 2

COBRA/TRAC - A Thermal-Hydraulics Code for Transient Analysis of Nuclear Reactor Vessels and Primary Coolant Systems

COBRA/TRAC Numerical Solution Methods

Prepared by M. J. Thurgood, T. L. George

Pacific Northwest Laboratory
Operated by
Battelle Memorial Institute

Prepared for
U.S. Nuclear Regulatory
Commission

NOTICE

This report was prepared as an account of work sponsored by an agency of the United States Government. Neither the United States Government nor any agency thereof, or any of their employees, makes any warranty, expressed or implied, or assumes any legal liability of responsibility for any third party's use, or the results of such use, of any information, apparatus, product or process disclosed in this report, or represents that its use by such third party would not infringe privately owned rights.

Availability of Reference Materials Cited in NRC Publications

Most documents cited in NRC publications will be available from one of the following sources:

1. The NRC Public Document Room, 1717 H Street, N.W.
Washington, DC 20555
2. The NRC/GPO Sales Program, U.S. Nuclear Regulatory Commission,
Washington, DC 20555
3. The National Technical Information Service, Springfield, VA 22161

Although the listing that follows represents the majority of documents cited in NRC publications, it is not intended to be exhaustive.

Referenced documents available for inspection and copying for a fee from the NRC Public Document Room include NRC correspondence and internal NRC memoranda; NRC Office of Inspection and Enforcement bulletins, circulars, information notices, inspection and investigation notices; Licensee Event Reports; vendor reports and correspondence; Commission papers; and applicant and licensee documents and correspondence.

The following documents in the NUREG series are available for purchase from the NRC/GPO Sales Program: formal NRC staff and contractor reports, NRC-sponsored conference proceedings, and NRC booklets and brochures. Also available are Regulatory Guides, NRC regulations in the *Code of Federal Regulations*, and *Nuclear Regulatory Commission Issuances*.

Documents available from the National Technical Information Service include NUREG series reports and technical reports prepared by other federal agencies and reports prepared by the Atomic Energy Commission, forerunner agency to the Nuclear Regulatory Commission.

Documents available from public and special technical libraries include all open literature items, such as books, journal and periodical articles, and transactions. *Federal Register* notices, federal and state legislation, and congressional reports can usually be obtained from these libraries.

Documents such as theses, dissertations, foreign reports and translations, and non-NRC conference proceedings are available for purchase from the organization sponsoring the publication cited.

Single copies of NRC draft reports are available free upon written request to the Division of Technical Information and Document Control, U.S. Nuclear Regulatory Commission, Washington, DC 20555.

Copies of industry codes and standards used in a substantive manner in the NRC regulatory process are maintained at the NRC Library, 7920 Norfolk Avenue, Bethesda, Maryland, and are available there for reference use by the public. Codes and standards are usually copyrighted and may be purchased from the originating organization or, if they are American National Standards, from the American National Standards Institute, 1430 Broadway, New York, NY 10018.

COBRA/TRAC - A Thermal-Hydraulics Code for Transient Analysis of Nuclear Reactor Vessels and Primary Coolant Systems

COBRA/TRAC Numerical Solution Methods

Manuscript Completed: November 1982
Date Published: March 1983

Prepared by
M. J. Thurgood, T. L. George

Pacific Northwest Laboratory
Richland, WA 99352

Prepared for
Division of Accident Evaluation
Office of Nuclear Regulatory Research
U.S. Nuclear Regulatory Commission
Washington, D.C. 20555
NRC FIN B2391

ABSTRACT

The COBRA/TRAC computer program has been developed to predict the thermal-hydraulic response of nuclear reactor primary coolant systems to small and large break loss-of-coolant accidents and other anticipated transients. The code solves the compressible three-dimensional, two-fluid, three-field equations for two-phase flow in the reactor vessel. The three fields are the vapor field, the continuous liquid field, and the liquid drop field. A five-equation drift flux model is used to model fluid flow in the primary system piping, pressurizer, pumps, and accumulators. The heat generation rate of the core is specified by input and no reactor kinetics calculations are included in the solution. This volume describes the finite-difference equations and the numerical solution methods used to solve these equations. It is directed toward the user who is interested in gaining a more complete understanding of the numerical methods used to obtain a solution to the hydrodynamic equations.

CONTENTS

ACKNOWLEDGEMENTS.....	vii
NOMENCLATURE.....	ix
1.0 INTRODUCTION.....	1.1
2.0 THREE-FIELD CONSERVATION EQUATIONS.....	2.1
2.1 COMPUTATIONAL MESH AND VARIABLE PLACEMENT.....	2.1
2.2 FINITE-DIFFERENCE EQUATIONS.....	2.5
2.2.1 Mass Equations.....	2.6
2.2.2 Fluid Energy Equations.....	2.8
2.2.3 Momentum Equations in the Vertical Direction.....	2.10
2.2.4 Momentum Equations in the Transverse Directions.....	2.15
3.0 SOURCE, VISCOUS, AND TURBULENCE TERMS.....	3.1
3.1 MASS, ENERGY, AND MOMENTUM SOURCE TERMS.....	3.1
3.1.1 Vessel Connection Source Terms.....	3.1
3.1.2 Boundary Condition Source Terms.....	3.5
3.2 VISCOUS AND TURBULENT SHEAR STRESS TENSORS AND HEAT FLUX VECTORS.....	3.7
3.3 Velocity Gradient for Point A.....	3.13
4.0 NUMERICAL SOLUTION.....	4.1
4.1 SOLUTION OF THE MOMENTUM EQUATIONS.....	4.1
4.2 LINEARIZATION OF THE MASS AND ENERGY EQUATIONS.....	4.3
4.3 SOLUTION OF THE SYSTEM PRESSURE MATRIX.....	4.8
4.4 UNFOLDING OF INDEPENDENT AND DEPENDENT VARIABLES.....	4.9
4.5 PRESSURE EQUATION FOR CELLS CONNECTED TO ONE-DIMENSIONAL COMPONENTS.....	4.10
4.6 TIME STEP CONTROL.....	4.11
REFERENCES	R.1

FIGURES

2.1	Basic Mesh Cell.....	2.2
2.2	Variable Mesh.....	2.3
2.3	Mesh Cell for Vertical Velocities.....	2.4
2.4	Mesh Cell for Transverse Velocities.....	2.4
3.1	Coordinate System and Nomenclature.....	3.8
3.2	Vertical Stresses Acting on Vertical Momentum Cell.....	3.12
3.3	Velocity Gradient for Point A.....	3.13

ACKNOWLEDGEMENTS

COBRA/TRAC is the result of the efforts of a number of people. We wish to acknowledge the main contributors and to express our appreciation to those who have offered their advice and suggestions.

The main contributors to the program are listed below.

Fluid Dynamics:	M. J. Thurgood, T. L. George, and T. E. Guidotti
Heat Transfer:	J. M. Kelly and R. J. Kohrt
Turbulence Model:	K. R. Crowell
Graphics and Programming:	A. S. Koontz
Simulations:	K. L. Basehore, S. H. Bian, J. M. Cuta, R. J. Kohrt, G. A. Sly, and C. A. Wilkins
One-Dimensional Components and Code Architecture:	Members of the TRAC Code Development Group at LANL

We wish to thank Dr. S. Fabric of the U.S. Nuclear Regulatory Commission for his patience, support, and suggestions during this large undertaking. We also wish to thank Drs. Tong, Shotkin, Han and Zuber of the U.S. Nuclear Regulatory Commission and members of the Advanced Code Review Group for their many helpful suggestions. We also express our gratitude to our manager, Dr. D. S. Trent, for his support, and Peggy Snyder and Cathy Darby for their lead roles in typing this report.

NOMENCLATURE

A	area
ALAT	area through which a vertical velocity convects transverse momentum
Cp	specific heat at constant pressure
$\underline{\underline{D}}$	deformation tensor
$\underline{\underline{D}}^*$	deleted deformation tensor
e	internal energy
E	error
F	mass flow rate
\underline{F}	total force due to viscous and turbulent shear stress
$\underline{\underline{F}}$	anisotropy tensor
FA	flow area for connection to the vessel
\underline{g}	gravitational acceleration
H	heat transfer coefficient
h	enthalpy
h_{fg}	enthalpy of vaporization
\underline{i}	unit vector in the x direction
\underline{j}	unit vector in the y direction
K	drag coefficient
\underline{k}	unit vector in the z direction
ℓ	mixing length
$\Delta \ell$	transverse length increment
n	unit normal vector
NA	number of connections to top of mesh cell
NB	number of connections to bottom of mesh cell
NCA	number of connections to top of transverse momentum cell
NCB	number of connections to bottom of transverse momentum cell
NCON	total number of connections to a cell
NKA	number of connections to top half of vertical momentum cell
NKB	number of connections to bottom half of vertical momentum cell
NKII	number of transverse connections to the II face of a transverse momentum cell

NKJJ	number of transverse connections to the JJ face of a transverse momentum cell
NKK	Total number of transverse connections to a scalar mesh cell
NG	number of transverse connections to a transverse momentum cell that are orthogonal to the transverse momentum cell velocity
NVCONIL	number of connections to the vessel in any one piping loop
P	pressure
q	interfacial heat flux
Q	sensible heat
S	width of transverse connection
S	source
S	net entrainment rate
T	turbulent and viscous shear stress terms
$\underline{\underline{T}}$	stress tensor
$\underline{\underline{T}}^T$	Reynolds stress tensor
Δt	time increment
U	vertical velocity
V	transverse velocity in Y direction
W	transverse velocity in Z direction
Δx	mesh vertical length increment

Greek Symbols

α	volume fraction — <i>void fraction?</i>
δ	linear variation of
Γ	net rate of vapor generation
ϵ	thermal diffusivity
ϵ^T	turbulent thermal diffusivity
η	fraction of vapor generation coming from the entrained liquid
μ	viscosity
μ^T	turbulent viscosity
ρ	density
$\underline{\underline{g}}$	fluid-fluid stress tensor
τ_i	interfacial drag force

Subscripts

B	bulk property
C	condensation
c	continuity cell
CE	entrained drop mass error
CL	continuous liquid mass error
CV	vapor mass error
ce	source of entrained liquid mass
cl	source of continuous liquid mass
cv	source of vapor mass
CONV	convection area
D	deposition or de-entrainment
E	evaporation or entrainment
e	entrained drop phase
el	liquid energy source
ev	vapor energy source
EL	liquid energy error
EV	vapor energy error
f	saturated liquid
g	saturated vapor
h	energy mixing length
I	counter on vertical stacks (channels) of computational mesh cells
i	interfacial
IA	counter on connections to top of transverse momentum cell
IB	counter on connections to bottom of transverse momentum cell
II	mesh cell on the upstream side of a transverse momentum cell
J	vertical level for scalar (mass, energy) mesh cell
j	vertical level for vertical momentum mesh cell
JJ	mesh cell on the down stream side of a transverse momentum cell
K	counter on transverse connections between vertical stacks of mesh cells
k	phase k
KA	counter on connections to top of mesh cell
KB	counter on connections to bottom of mesh cell

L	counter on transverse connections to a cell
ℓ	continuous liquid phase
LA	counter on transverse connections to top of vertical momentum cell
LB	counter on transverse connections to bottom of vertical momentum cell
m	mixture property
m	momentum mixing length
m	momentum cell
me	entrained liquid momentum source
$m\ell$	continuous liquid momentum source
mv	vapor momentum source
p	pipe
r	relative velocity
sink	related to a pressure sink boundary condition
v	vapor phase
ve	drag between vapor and drops
$v\ell$	drag between vapor and continuous liquid
w	wall

Superscripts

n	new time value
T	turbulent
t	transpose
'	per unit length
*	donor cell quantity

COBRA/TRAC - A THERMAL-HYDRAULICS CODE FOR TRANSIENT ANALYSIS
OF NUCLEAR REACTOR VESSELS AND PRIMARY COOLANT SYSTEMS
VOLUME 2: COBRA/TRAC NUMERICAL SOLUTION METHODS

1.0 INTRODUCTION

The COBRA/TRAC computer program was developed to predict the thermal-hydraulic response of nuclear reactor primary coolant systems to small and large break loss-of-coolant accidents and other anticipated transients. It was derived from the merging of COBRA-TF and TRAC-PD2 (Ref. 1).

The COBRA-TF computer code provides a two-fluid, three-field representation of two-phase flow. Each field is treated in three dimensions and is compressible. Continuous vapor, continuous liquid, and entrained liquid drop are the three fields. The conservation equations for each of the three fields and for heat transfer from and within the solid structures in contact with the fluid are solved using a semi-implicit finite-difference numerical technique on an Eulerian mesh. COBRA-TF features extremely flexible noding for both the hydrodynamic mesh and the heat transfer solution. This flexibility provides the capability to model the wide variety of geometries encountered in vertical components of nuclear reactor primary systems.

TRAC-PD2 is a systems code designed to model the behavior of the entire reactor primary system. It features special models for each component in the system. These include accumulators, pumps, valves, pipes, pressurizers, steam generators, and the reactor vessel. With the exception of the reactor vessel, the thermal-hydraulic response of these components to transients is treated with a five-equation drift flux representation of two-phase flow. The vessel component of TRAC-PD2 is somewhat restricted in the geometries that can be modeled and cannot treat the entrainment of liquid drops from the continuous liquid phase directly.

The TRAC-PD2 vessel module was removed and COBRA-TF implemented as the new vessel component in TRAC-PD2. The resulting code is COBRA/TRAC. The vessel component in COBRA/TRAC has the extended capabilities provided by the

three-field representation of two-phase flow and the flexible noding. The code has been assessed against a variety of two-phase flow data from experiments conducted to simulate important phenomena anticipated during postulated accidents and transients in light water nuclear reactors.

The documentation of the COBRA/TRAC program is contained in five separate volumes. Volume 1 contains a description of the basic three-field conservation equations and constitutive models used in the vessel component (COBRA-TF).

The constitutive relations included in COBRA-TF include state-of-the-art physical models for the interfacial mass transfer, the interfacial drag forces, the liquid and vapor wall drag, the wall and interfacial heat transfer, the rate of entrainment and de-entrainment, and the thermodynamic properties of water. In addition, a mixing length turbulence model has been included as an option. Volume 2 contains a description of the finite-difference equations for the vessel and the numerical techniques used to solve these equations. The coupling between the TRAC-PD2 equations and the COBRA-TF vessel equations is also described. Volume 3 is the Users' Manual and contains line-by-line input instructions for COBRA/TRAC. Volume 4 is the Assessment Manual, containing the results of simulations run to assess the performance of the code. Volume 5 is the Programmers' Guide and provides information on the basic code structure and auxiliary programs required to run COBRA/TRAC.

This volume, Numerical Solution Methods, describes the finite-difference equations and the numerical solution methods used to solve these equations. The finite-difference equations are presented in Sections 2 and 3. The numerical solution method is described in Section 4.

2.0 THREE-FIELD CONSERVATION EQUATIONS

The three-field conservation equations for multidimensional flow in the vessel component (COBRA-TF) are presented in Volume 1 of this manual. The reader should refer to Volume 1 for a more complete discussion of these equations and a description of the physical models required for their closure. The finite-difference form of these equations will be presented here and the term by term correspondence between the conservation equations and the finite-difference equations will be pointed out.

The finite-difference equations are written in a semi-implicit form using donor cell differencing for the convected quantities. Since a semi-implicit form is used, the time step, Δt , is limited by the material Courant limit

$$\Delta t < \left| \frac{\Delta x}{V} \right| \quad (2.1)$$

where Δx is the mesh spacing and V is the fluid velocity.

The finite-difference equations are written such that they may be solved on Cartesian coordinates or using the subchannel formulation in which some of the convective terms in the transverse momentum equations are neglected and idealistic assumptions are made concerning the shape of the transverse momentum control volumes.

The computational mesh and finite-difference equations are described using the generalized subchannel notations. These equations are equivalent to the three-dimensional Cartesian equations when the limiting assumptions of the subchannel formulation are not used and the mesh is arranged on a rectangular grid (see Volume 1, Section 2).

2.1 COMPUTATIONAL MESH AND VARIABLE PLACEMENT

The equations are solved using a staggered-difference scheme where the velocities are obtained at the mesh cell faces and the state variables such as pressure, density, enthalpy, and void fraction are obtained at the cell center. The mesh cell is characterized by its cross-sectional area, A , its

height, Δx , and the width of its connection with adjacent mesh cells, S . The basic mesh cell is shown in Figure 2.1. The basic mesh cell may be used to model any one, two, or three-dimensional region. The dimensionality of the flow is dependent upon the number of faces on the cell that connect with adjacent mesh cells.

The size of a mesh cell used to model the flow field inside of a reactor vessel is generally quite large because the volume of the reactor vessel is very large and the cost of using a fine mesh in solving the two-fluid equations for the whole vessel would be prohibitive. However, many important flow paths and flow phenomena may be overlooked when a large mesh size is used in some areas of the vessel. This can be minimized by allowing a variable mesh size within the vessel. A finer mesh can be used in areas where a more detailed calculation of the flow field is required. The vessel component has been set up to allow such a variable mesh size. Examples of the flexibility this allows in modeling various geometries are given in the users' manual (Volume 3) and the applications manual (Volume 5). The variable

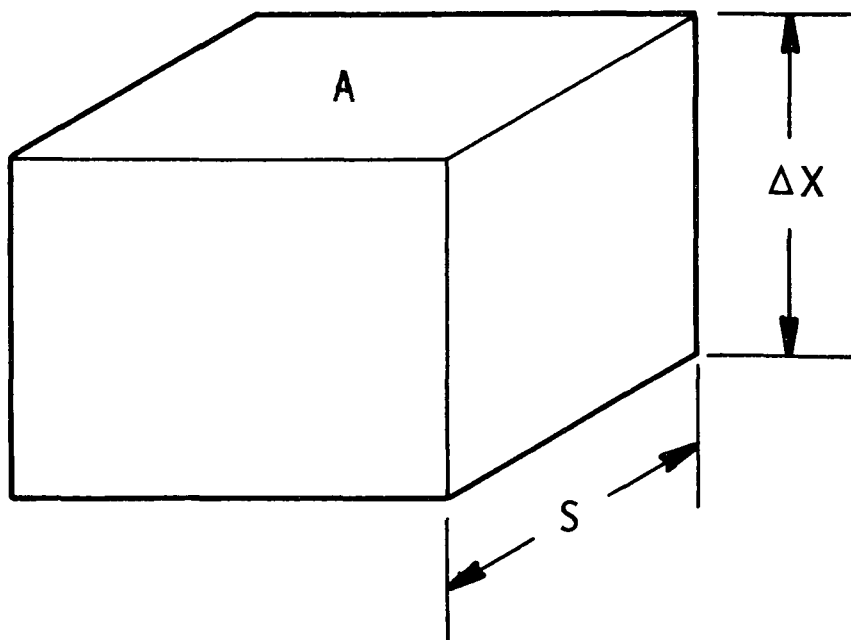


FIGURE 2.1. Basic Mesh Cell

mesh is formed by connecting two or more cells to any or all of the faces of a mesh cell, as illustrated in Figure 2.2. A single mesh cell with area A_1 is shown connected to four mesh cells above it with areas A_2 , A_3 , etc. These four mesh cells may connect through transverse connections S_2 , S_3 , etc., to allow transverse flow in that region, or they may not connect to each other forming one or more one-dimensional flow paths that connect to mesh cell 1. A more detailed discussion of the mesh is given in the Users' Manual (Volume 3).

The mesh cells shown in Figures 2.1 and 2.2 represent the mesh for the scalar continuity and energy equations. The momentum equations are solved on a staggered mesh where the momentum mesh cell is centered on the scalar mesh cell surface. The mesh cell for vertical velocities is shown in Figure 2.3, and that for transverse velocities in Figure 2.4.

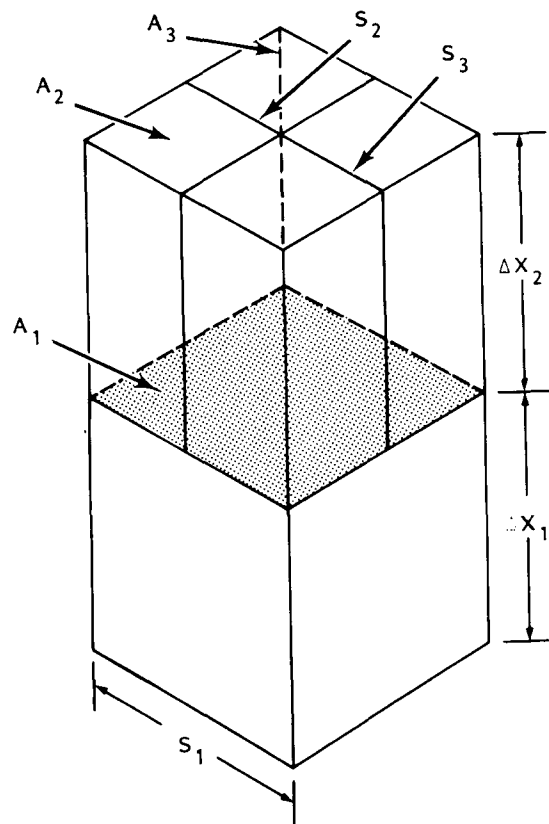


FIGURE 2.2. Variable Mesh

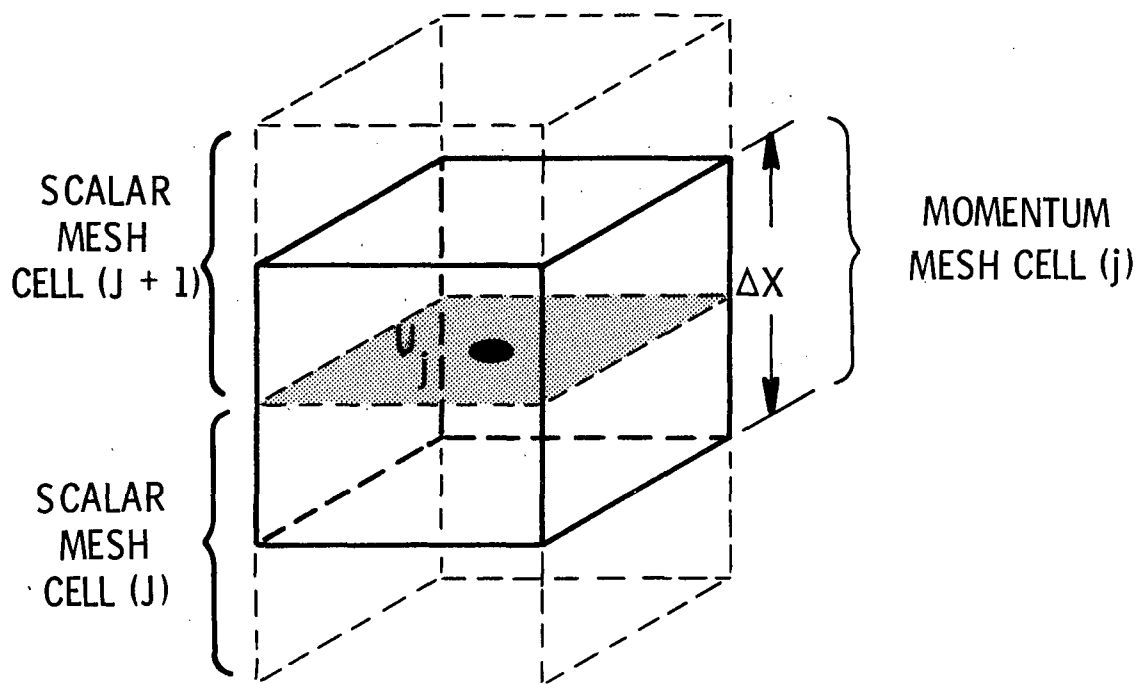


FIGURE 2.3. Mesh Cell for Vertical Velocities

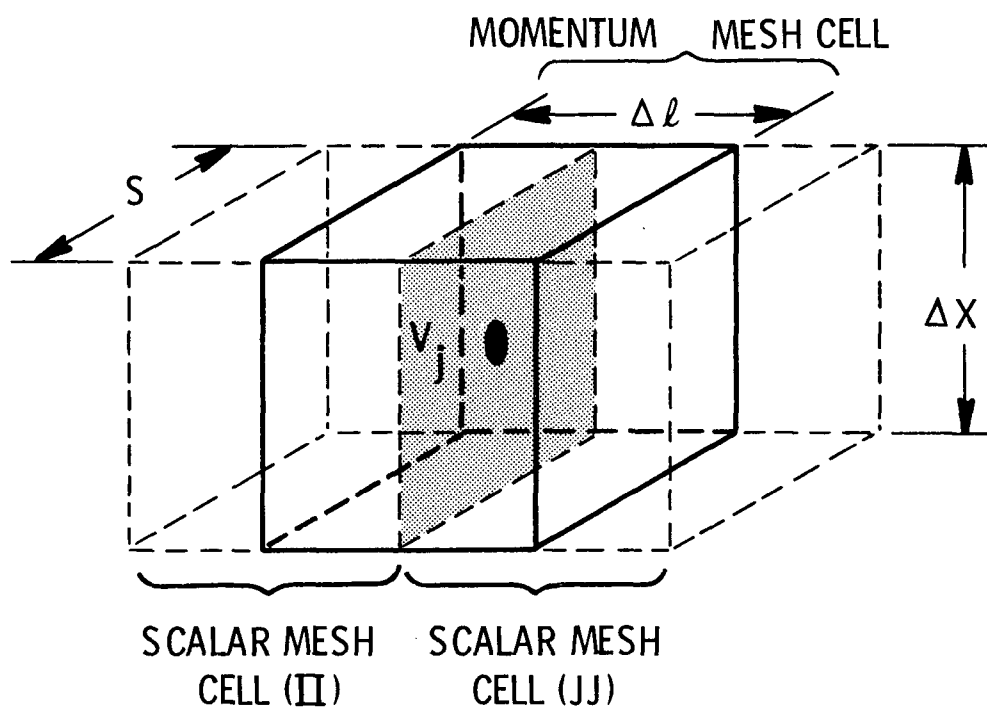


FIGURE 2.4. Mesh Cell for Transverse Velocities

The vertical velocities are subscripted with I and j where I identifies the location of the mesh cell within the horizontal plane and j identifies its vertical location. The mesh cells for the scalar equations carry the same subscripts, but their mesh cell centers lie a distance $\Delta x/2$ below the mesh cell center for the correspondingly subscripted velocity and are denoted by the capital letter J in the discussion below.

Transverse velocities are subscripted with k and J where k identifies the location of the mesh cell in the horizontal plane and J identifies its vertical location. The node centers for the scalar equations and transverse momentum equations lie in the same horizontal plane.

The finite-difference equations are written based on the mesh as defined above using this subscripting convention.

2.2 FINITE-DIFFERENCE EQUATIONS

The finite-difference equations follow. Quantities that are evaluated at the new time carry the superscript n and donor cell quantities carry the superscript $*$. Those quantities that have the superscript $*$ or no superscript are evaluated at the old time and form the explicit portions of the equations. The corresponding term in the conservation equation for each term in the finite-difference equation is provided in the brackets below each equation, along with a verbal description of the term. The subscripts I and k are assumed to be obvious and are not shown.

2.2.1 Mass Equations

Vapor Mass Equation:

$$\begin{aligned} \frac{[(\alpha_v \rho_v)_J^n - (\alpha_v \rho_v)_J]}{\Delta t} A_{C_J} &= \frac{\sum_{KB=1}^{NB} [(\alpha_v \rho_v)^* U_{v,j-1}^n A_{m,j-1}]_{KB} - \sum_{KA=1}^{NA} [(\alpha_v \rho_v)^* U_{v,j}^n A_{m,j}]_{KA}}{\Delta x_J} \\ &+ \sum_{L=1}^{NKK} S_L [(\alpha_v \rho_v)^* v_{v,L}^n]_J + \frac{r_J^n}{\Delta x_J} + \frac{S_{cv,J}^n}{\Delta x_J} \end{aligned} \quad (2.2)$$

Liquid Mass Equation:

$$\begin{aligned} \frac{[(\alpha_\ell \rho_\ell)_J^n - (\alpha_\ell \rho_\ell)_J]}{\Delta t} A_{C_J} &= \frac{\sum_{KB=1}^{NB} [(\alpha_\ell \rho_\ell)^* U_{\ell,j-1}^n A_{m,j-1}]_{KB} - \sum_{KA=1}^{NA} [(\alpha_\ell \rho_\ell)^* U_{\ell,j}^n A_{m,j}]_{KA}}{\Delta x_J} \\ &+ \sum_{L=1}^{NKK} S_L [(\alpha_\ell \rho_\ell)^* v_{\ell,L}^n]_J - \frac{(1-\eta) r_J^n}{\Delta x_J} - \frac{S_J}{\Delta x_J} + \frac{S_{c\ell,J}^n}{\Delta x_J} \end{aligned} \quad (2.3)$$

Entrained Liquid Mass Equation:

$$\begin{aligned} \frac{[(\alpha_e \rho_\ell)_J^n - (\alpha_e \rho_\ell)_J]}{\Delta t} A_{C_J} &= \frac{\sum_{KB=1}^{NB} [(\alpha_e \rho_\ell)^* U_{e,j-1}^n A_{m,j-1}]_{KB} - \sum_{KA=1}^{NA} [(\alpha_e \rho_\ell)^* U_{e,j}^n A_{m,j}]_{KA}}{\Delta x_J} \\ &+ \sum_{L=1}^{NKK} S_L [(\alpha_e \rho_\ell)^* v_{e,L}^n]_J - \frac{\eta r_J^n}{\Delta x_J} + \frac{S_J}{\Delta x_J} + \frac{S_{ce,J}^n}{\Delta x_J} \end{aligned} \quad (2.4)$$

$$\begin{aligned}
& \left[\begin{array}{c} \text{Rate of Change of Mass} \\ A \frac{\partial}{\partial t} (\alpha_k \rho_k) \end{array} \right] = - \left[\begin{array}{c} \text{Rate of Mass Efflux in the Vertical} \\ \text{Direction} \\ \frac{\partial \alpha_k \rho_k U_k}{\partial x} A \end{array} \right] \\
& - \left[\begin{array}{c} \text{Rate of Mass Efflux in} \\ \text{the Transverse Direction} \\ \sum_L (\alpha_k \rho_k V_k)_L S_L \end{array} \right] + \left[\begin{array}{c} \text{Rate of Creation} \\ \text{of Vapor Mass Due} \\ \text{to Phase Change} \\ \Gamma'_k \end{array} \right] + \left[\begin{array}{c} \text{Mass Efflux} \\ \text{Due to} \\ \text{Entrainment} \\ S' \end{array} \right] + \left[\begin{array}{c} \text{Phase} \\ \text{Source} \\ \text{Term} \\ S_c \end{array} \right]
\end{aligned}$$

The reader should refer to the nomenclature list for the definition of each of the variables. The rate of mass efflux in the transverse direction is given as the sum of the mass entering the cell through all transverse connections to all of the faces. The total number of transverse connections to the cell is NKK. The rate of mass efflux in the vertical direction is given as the sum of the mass entering (or leaving) the cell through all vertical connections to the top and bottom of the cell. The total number of connections to the top of the cell is NA and the number of connections to the bottom of the cell is NB.

The velocity in each of the convection terms is taken to be the new time value while the convected quantity, in this case $(\alpha_k \rho_k)^*$, is taken at the old time. The mass creation term is evaluated at the new time. However, it consists of an implicit and explicit part. The rate of mass generation due to phase change, Γ_J , is given by

$$\Gamma_J^n = - \frac{(H_i A_i)_\ell (h_f - h_\ell)^n}{C_{p_\ell} h_{fg}} - \frac{(H_i A_i)_v (h_g - h_v)^n}{C_{p_v} h_{fg}} \quad (2.5)$$

The product of the interfacial area and heat transfer coefficient, the specific heats, and the heat of vaporization are all evaluated at the old time value and form the explicit portion of the mass creation term, while the

enthalpies are evaluated at the new time value forming the implicit portion. This term is also multiplied by the ratio $(1-\alpha_V^n)/(1-\alpha_V)$ for vaporization or α_V^n/α_V for condensation. This is done to provide an implicit ramp that will cause the interfacial area to go to zero as all of the donor phase is depleted. An explicit ramp is also applied to the product $(H_i A_i)$ to cause it to go to zero as the volume fraction of the donor phase approaches zero. The entrainment rate S is explicit and is also multiplied by implicit and explicit ramps that force it to zero as the donor liquid phase is depleted.

The last term in the equations is the phase mass source term and is evaluated at the new time. This term accounts for sources of vapor mass that are exterior to the vessel mesh. These sources include one-dimensional component connections such as pipes, mass injection boundary conditions, and pressure boundary conditions. These source terms will be defined in the next section.

2.2.2 Fluid Energy Equations

Vapor Energy Equation:

$$\frac{[(\alpha_V \rho_V h_V)_J^n - (\alpha_V \rho_V h_V)_J] A_{C_J}}{\Delta t} =$$

$$\frac{\sum_{KB=1}^{NB} [(\alpha_V \rho_V h_V)^* U_{V_{j-1}}^n A_{m_{j-1}}]_{KB} - \sum_{KA=1}^{NA} [(\alpha_V \rho_V h_V)^* U_{V_j}^n A_{m_j}]_{KA}}{\Delta x_J} \quad (2.6)$$

$$+ \sum_{L=1}^{NKK} S_L [(\alpha_V \rho_V h_V)^* V_{V_L}^n]_J + \frac{r_J^n h_{gJ}^n}{\Delta x_J} + \frac{q_{ivJ}^n}{\Delta x_J} + \frac{Q_{vJ}}{\Delta x_J} + \frac{S_{ev}^n}{\Delta x_J} + \frac{Q_{vJ}^T}{\Delta x_J} + \frac{\alpha_{V_J} (P^n - P)_J A_{C_J}}{\Delta t}$$

Liquid Energy Equation:

$$\frac{\{[(\alpha_l + \alpha_e)\rho_l h_l]_J^n - [(\alpha_e + \alpha_l)\rho_l h_l]_J\} A_{cJ}}{\Delta t} =$$

$$\begin{aligned} & \frac{1}{\Delta x_J} \left\{ \sum_{KB=1}^{NB} [(\alpha_l \rho_l h_l)^* U_{l,j-1}^n A_{m,j-1} + (\alpha_e \rho_l h_l)^* U_{e,j-1}^n A_{m,j-1}]_{KB} - \sum_{KA=1}^{NA} [(\alpha_l \rho_l h_l)^* U_{l,j}^n A_{m,j} \right. \\ & \left. + (\alpha_e \rho_l h_l)^* U_{e,j}^n A_{m,j}]_{KA} \right\} + \sum_{L=1}^{NKK} S_L [(\alpha_l \rho_l h_l)^* V_{l,L}^n + (\alpha_e \rho_l h_l)^* V_{e,L}^n]_J \\ & - \frac{\Gamma_J^n h_{fJ}^n}{\Delta x_J} + \frac{q_{iJ}^n}{\Delta x_J} + \frac{Q_{lJ}}{\Delta x_J} + \frac{S_{eJ}^n}{\Delta x_J} + \frac{Q_{lJ}^T}{\Delta x_J} + \frac{\alpha_{lJ} (P^n - P)_J A_{cJ}}{\Delta t} \end{aligned} \quad (2.7)$$

$$\left[\begin{array}{c} \text{Rate of Change of Enthalpy} \\ A \frac{\partial}{\partial t} (\alpha_k \rho_k h_k) \end{array} \right] = - \left[\begin{array}{c} \text{Rate of Efflux of Enthalpy} \\ \text{in the Vertical Direction} \\ \frac{\partial}{\partial x} (\alpha_k \rho_k h_k U_k) \end{array} \right]$$

$$\begin{aligned} & + \left[\begin{array}{c} \text{Rate of Efflux of Enthalpy} \\ \text{in the Transverse Direction} \\ \sum_L (\alpha_k \rho_k h_k V_k)_L S_L \end{array} \right] + \left[\begin{array}{c} \text{Energy Efflux Due To Mass} \\ \text{Transfer Between Fields} \\ \Gamma_k' h_k \end{array} \right] \\ & + \left[\begin{array}{c} \text{Interfacial Heat Transfer} \\ q_i' \end{array} \right] + \left[\begin{array}{c} \text{Heat Addition} \\ \text{from Solid} \\ Q_w \end{array} \right] + \left[\begin{array}{c} \text{Fluid Convection} \\ \text{and Turbulent} \\ \text{Heat Flux} \\ \nabla \cdot [\alpha_k (\underline{q}_k + \underline{q}_k)^T] \end{array} \right] + \left[\begin{array}{c} \text{Pressure} \\ \text{Derivative} \\ \alpha \frac{\partial P}{\partial t} \end{array} \right] \end{aligned}$$

Again, the rate of energy efflux in the transverse direction is the sum of all transverse connections on all faces of the cell and that in the vertical direction is the sum of all connections to the top and bottom of the cell. New time velocities convect the donor cell $(\alpha_k \rho_k h_k)^*$ which is evaluated using old time values. New time enthalpies are convected in the phase change term. The interfacial heat transfer term, like the vapor generation term, has an implicit temperature difference and an explicit heat transfer coefficient and interfacial area. The wall heat transfer is explicit. The energy source terms corresponding to the mass source terms will be defined in the next section. The fluid conduction and turbulent heat flux are explicit and will be expanded in the next section.

2.2.3 Momentum Equations in the Vertical Direction

Vapor Phase:

$$\frac{[(\alpha_v \rho_v U_v)_j^n - (\alpha_v \rho_v U_v)_j] A_{m_j}}{\Delta t} = \sum_{KB=1}^{NB} \frac{[(\alpha_v \rho_v U_v)^* U_{v_j}]_{KB} A_{m_{KB}}}{\Delta x_j} - \sum_{KA=1}^{NA} \frac{[(\alpha_v \rho_v U_v)^* U_{v_{j+1}}]_{KA} A_{m_{KA}}}{\Delta x_j} + \sum_{LB=1}^{NKB} [(\alpha_v \rho_v U_v)^* v_{v_j}]_{LB} \frac{S_{LB}}{2} \quad (2.8)$$

$$+ \sum_{LA=1}^{NKA} [(\alpha_v \rho_v U_v)^* v_{v_{j+1}}]_{LA} \frac{S_{LA}}{2} - (\alpha_v \rho_v)_j g A_{m_j} - \frac{(P_{j+1} - P_j)^n}{\Delta x_j} \alpha_{v_j} A_{m_j}$$

$$- K_{vj} (2U_{vj}^n - U_{vj}) - K_{vlj} [2(U_v - U_{lj})_j^n - (U_v - U_{lj})_j] - K_{vej} [2(U_v - U_e)_j^n - (U_v - U_e)_j]$$

$$- \frac{[r_C U_v - (1-n)r_E U_{lj} - nr_E U_e]_j}{\Delta x_j} + \frac{S_{mvj}}{\Delta x_j} + T_{vj}^T$$

Liquid Phase:

$$\frac{[(\alpha_{lj} \rho_{lj} U_{lj})_j^n - (\alpha_{lj} \rho_{lj} U_{lj})_j] A_{mj}}{\Delta t} = \frac{\sum_{KB=1}^{NB} [(\alpha_{lj} \rho_{lj} U_{lj})^* U_{lj}]_{KB} A_{mKB}}{\Delta x_j}$$

$$- \frac{\sum_{KA=1}^{NA} [(\alpha_{lj} \rho_{lj} U_{lj})^* U_{lj+1}]_{KA} A_{mKA}}{\Delta x_j} + \sum_{LB=1}^{NKB} [(\alpha_{lj} \rho_{lj} U_{lj})^* v_{lj}]_{LB} \frac{S_{LB}}{2} \quad (2.9)$$

$$+ \sum_{LA=1}^{NKA} [(\alpha_{lj} \rho_{lj} U_{lj})^* v_{lj+1}]_{LA} \frac{S_{LA}}{2} - (\alpha_{lj} \rho_{lj})_j g A_{mj}$$

$$- \frac{(P_{j+1} - P_j)^n}{\Delta x_j} \alpha_{lj} A_{mj}$$

$$- K_{lj} (2U_{lj}^n - U_{lj}) + K_{vlj} [2(U_v - U_{lj})_j^n - (U_v - U_{lj})_j] + \frac{(1-n) [r_C U_v - r_E U_{lj}]_j}{\Delta x_j}$$

$$+ \frac{(S_D^{U_e} - S_E^{U_e})_j}{\Delta x_j} + \frac{S_{m\ell_j}}{\Delta x_j} + T_{\ell_j}^T$$

Entrained Liquid Phase:

$$\frac{[(\alpha_{e\ell} U_e)_j^n - (\alpha_{e\ell} U_e)_j] A_{mj}}{\Delta t} = \frac{\sum_{KB=1}^{NB} [(\alpha_{e\ell} U_e)^*_{U_{e_j}}]_{KB} A_{m_{KB}}}{\Delta x_j}$$

$$- \frac{\sum_{KA=1}^{NA} [(\alpha_{e\ell} U_e)^*_{U_{e_{j+1}}}]_{KA} A_{m_{KA}}}{\Delta x_j} + \sum_{LB=1}^{NKB} [(\alpha_{e\ell} U_e)^*_{v_{e_j}}]_{LB} \frac{S_{LB}}{2}$$

$$+ \sum_{LA=1}^{NKA} [(\alpha_{e\ell} U_e)^*_{v_{e_{j+1}}}]_{LA} \frac{S_{LA}}{2} - (\alpha_{e\ell})_j g A_{mj} \quad (2.10)$$

$$- \frac{(P_{j+1} - P_j)^n}{\Delta x_j} \alpha_{e_j} A_{mj}$$

$$- K_{e_j} (2U_{e_j}^n - U_{e_j}) + K_{ve_j} [2(U_v - U_e)_j^n - (U_v - U_e)_j] + \frac{\eta[r_C^{U_v} - r_E^{U_e}]_j}{\Delta x_j}$$

$$- \frac{(S_D^{U_e} - S_E^{U_e})_j}{\Delta x_j} - \frac{S_{me_j}}{\Delta x_j}$$

$$\begin{aligned}
& \left[\begin{array}{l} \text{Rate of Change} \\ \text{of Vertical} \\ \text{Momentum} \\ A \frac{\partial(\alpha_k \rho_k U_k)}{\partial t} \end{array} \right] = - \left[\begin{array}{l} \text{Rate of Efflux of Momentum at Bottom of Cell. Rate} \\ \text{of Efflux of Momentum at Top of Cell} \\ A \frac{\partial}{\partial x} (\alpha_k \rho_k U_k U_k) \end{array} \right] \\
& + \left[\begin{array}{l} \text{Rate of Efflux of Momentum in} \\ \text{the Transverse Direction} \\ \sum_L (\alpha_k \rho_k U_k V_k)_L S_L \end{array} \right] - \left[\begin{array}{l} \text{Gravitational} \\ \text{Force} \\ \alpha_k \rho_k g \end{array} \right] \\
& - \left[\begin{array}{l} \text{Pressure-Gradient} \\ \text{Force} \\ \alpha_k \frac{\partial p}{\partial x} \end{array} \right] - \left[\begin{array}{l} \text{Wall Shear} \\ \tau_w \end{array} \right] + \left[\begin{array}{l} \text{Interfacial Shear} \\ \tau_{i\,vl} + \tau_{i\,ve} \end{array} \right] \\
& + \left[\begin{array}{l} \text{Momentum Exchange Due} \\ \text{to Mass Transfer} \\ \text{Between Fields} \\ rU + sU \end{array} \right] + \left[\begin{array}{l} \text{Momentum Source Term} \\ S_m \end{array} \right] + \left[\begin{array}{l} \text{Viscous and Turbulent} \\ \text{Shear Stress} \\ \nabla \cdot [\alpha_k (\underline{\underline{\alpha}}_k + \underline{\underline{T}}_k^T)] \end{array} \right]
\end{aligned}$$

The rate of momentum efflux in the vertical direction is given as the sum of the momentum entering (or leaving) the cell through all vertical connections. The total number of momentum mesh cells facing the top of the

cell is NA and the total facing the bottom of the cell is NB. The rate of momentum efflux in the transverse direction is given as the sum of the momentum entering (or leaving) the cell through all transverse connections. The total number of transverse connections to the top half of the momentum cell is NKA. The total number of connections to the bottom half of the cell is NKB. In order to achieve stability with this semi-implicit formulation of the momentum equation, donor cell momentum, $(\alpha_k \rho_k U_k)^*$, is convected by the velocities at the momentum cell face through the area of the connections at the momentum cell face. A simple linear average between adjacent momentum cell velocities is taken to obtain the velocity at momentum cell faces since velocities are not computed at this location:

$$U_j = \frac{U_j + U_{j-1}}{2} \quad (2.11)$$

Likewise, linear averages are used to obtain other variables at a location where they are not defined. The void fraction of the momentum cell is given as

$$\alpha_j = \frac{\alpha_j + \alpha_{j+1}}{2} \quad (2.12)$$

and the density is given as

$$\rho_j = \frac{\rho_j + \rho_{j+1}}{2} \quad (2.13)$$

Velocities are obtained from the flow computed by the momentum equations, $(\alpha_k \rho_k U_k A_m)$, by dividing it by the momentum cell macroscopic density and momentum cell area

$$U_{k_j} = \frac{(\alpha_k \rho_k U_{k_m})_j}{(\alpha_k \rho_k A_m)_j} \quad (2.14)$$

The pressures in the pressure force term are taken at the new time as are the velocities in the wall shear and interfacial shear terms. The shear terms have been weighted toward the new time velocity by differencing them in the form: $K(2U^n - U)$. All other terms and variables are computed using old time values. The donor phase momentum is convected during mass exchange between fields. The explicit viscous and turbulent shear stresses will be expanded in the next section.

2.2.4 Momentum Equations in the Transverse Directions

Vapor Phase:

$$\begin{aligned} & \frac{[(\alpha_v \rho_v V_v)^n - (\alpha_v \rho_v V_v)]_J S_J \Delta x_J}{\Delta t} = \frac{\sum_{L=1}^{NKII} [(\alpha_v \rho_v V_v)_J^* V_{vL} S_L] \Delta x_J}{\Delta \ell_J} \\ & - \frac{\sum_{L=1}^{NKJJ} [(\alpha_v \rho_v V_v)_J^* V_{vL} S_L] \Delta x_J}{\Delta \ell_J} + \frac{\sum_{L=1}^{NG} [(\alpha_v \rho_v V_v)_J^* W_{vL} \frac{S_L}{2}] \Delta x_J}{\Delta \ell_J} \\ & + \frac{\sum_{IB=1}^{NCB} [(\alpha_v \rho_v V_v)_J^* U_{vIB} ALAT_{IB}] \Delta x_J}{\Delta \ell_J} - \frac{\sum_{IA=1}^{NCA} [(\alpha_v \rho_v V_v)_J^* U_{vIA} ALAT_{IA}] \Delta x_J}{\Delta \ell_J} \\ & - \frac{\alpha_{vII-JJ} (P_{JJ} - P_{II})^n S_J \Delta x_J}{\Delta \ell_J} - K_{vJ} (2V_{vJ}^n - V_{vJ}) - K_{v\ell J} [2(V_v - V_{\ell})_J^n - (V_v - V_{\ell})_J] \\ & - K_{veJ} [2(V_v - V_e)_J^n - (V_v - V_e)_J] - \frac{[\Gamma_C V_v - (1 - \eta) \Gamma_E V_{\ell} - \eta \Gamma_E V_e]_J}{\Delta \ell_J} + \frac{S_{mvJ}}{\Delta \ell_J} + T_{vJ}^T \end{aligned} \quad (2.15)$$

Liquid Phase:

$$\begin{aligned}
 & \frac{[(\alpha_{\ell \ell} \rho_{\ell} V_{\ell})^n - (\alpha_{\ell \ell} \rho_{\ell} V_{\ell})]_J S_J \Delta x_J}{\Delta t} = \frac{\sum_{L=1}^{NKII} [(\alpha_{\ell \ell} \rho_{\ell} V_{\ell})_J^* V_{\ell L} S_L] \Delta x_J}{\Delta \ell_J} \\
 & - \frac{\sum_{L=1}^{NKJJ} [(\alpha_{\ell \ell} \rho_{\ell} V_{\ell})_J^* V_{\ell L} S_L] \Delta x_J}{\Delta \ell_J} + \frac{\sum_{L=1}^{NG} [(\alpha_{\ell \ell} \rho_{\ell} V_{\ell})_J^* W_{\ell L} \frac{S_L}{2}] \Delta x_J}{\Delta \ell_J} \\
 & + \frac{\sum_{IB=1}^{NCB} [(\alpha_{\ell \ell} \rho_{\ell} V_{\ell})_J^* U_{\ell IB} ALAT_{IB}] \Delta x_J}{\Delta \ell_J} - \frac{\sum_{IA=1}^{NCA} [(\alpha_{\ell \ell} \rho_{\ell} V_{\ell})_J^* U_{\ell IA} ALAT_{IA}] \Delta x_J}{\Delta \ell_J} \quad (2.16) \\
 & - \frac{\alpha_{\ell II-JJ} (P_{JJ} - P_{II})^n S_J \Delta x_J}{\Delta \ell_J} - K_{\ell J} (2V_{\ell J}^n - V_{\ell J}) + K_{V \ell J} [2(V_V - V_{\ell})_J^n - (V_V - V_{\ell})_J] \\
 & + \frac{[(1-n)r_C V_V - (1-n)r_E V_{\ell}]_J}{\Delta \ell_J} + \frac{S_{m \ell J}}{\Delta \ell_J} + T_{\ell J}^T
 \end{aligned}$$

Entrained Liquid Phase:

$$\begin{aligned}
 & \frac{[(\alpha_{e\rho} v_e)^n - (\alpha_{e\rho} v_e)]_J S_J \Delta x_J}{\Delta t} = \frac{\sum_{L=1}^{NKII} [(\alpha_{e\rho} v_e)_J^* v_{eL} S_L] \Delta x_J}{\Delta \ell_J} \\
 & - \frac{\sum_{L=1}^{NKJJ} [(\alpha_{e\rho} v_e)_J^* v_{eL} S_L] \Delta x_J}{\Delta \ell_J} + \frac{\sum_{L=1}^{NG} [(\alpha_{e\rho} v_e)_J^* w_{eL} \frac{S_L}{2}] \Delta x_J}{\Delta \ell_J} \\
 & + \frac{\sum_{IB=1}^{NCB} [(\alpha_{e\rho} v_e)_J^* u_{eIB} ALAT_{IB}] \Delta x_J}{\Delta \ell_J} - \frac{\sum_{IA=1}^{NCA} [(\alpha_{e\rho} v_e)_J^* u_{eIA} ALAT_{IA}] \Delta x_J}{\Delta \ell_J} \quad (2.17) \\
 & - \frac{\alpha_{eII-JJ} (P_{JJ} - P_{II})^n S_J \Delta x_J}{\Delta \ell_J} - K_{eJ} (2v_{eJ}^n - v_{eJ}) + K_{veJ} [2(v_v - v_e)_J^n - (v_v - v_e)_J] \\
 & + \frac{(\eta_{\Gamma_C} v_v - \eta_{\Gamma_E} v_e)_J}{\Delta \ell_J} + \frac{S_{meJ}}{\Delta \ell_J}
 \end{aligned}$$

$$\begin{aligned}
& \left[\begin{array}{l} \text{Rate of Change} \\ \text{of Transverse} \\ \text{Momentum} \\ A \frac{\partial(\alpha_k \rho_k V_k)}{\partial t} \end{array} \right] = - \left[\begin{array}{l} \text{Rate of Transverse} \\ \text{Momentum Efflux} \\ \text{by Transverse Convection} \\ \frac{\partial(\alpha_k \rho_k V_k V_k A)}{\partial L} \end{array} \right] + \left[\begin{array}{l} \text{Rate of Transverse} \\ \text{Momentum Efflux} \\ \text{by Orthogonal} \\ \text{Transverse Convection} \\ \sum_{NK} (\alpha_k \rho_k V_k V_{k_{NK}} S'_{NK}) \end{array} \right] \\
& + \left[\begin{array}{l} \text{Rate of Transverse} \\ \text{Momentum Efflux} \\ \text{by Vertical Convection} \\ \frac{\partial}{\partial z} \alpha_k \rho_k V_k U_k A \end{array} \right] - \left[\begin{array}{l} \text{Pressure Gradient} \\ \text{Force} \\ \alpha_k A_k \frac{\partial P}{\partial L} \end{array} \right] - \left[\begin{array}{l} \text{Transverse} \\ \text{Wall Shear} \\ \tau''''_{wk_K} A_K \end{array} \right] \\
& + \left[\begin{array}{l} \text{Interfacial Drag} \\ \text{Between Vapor} \\ \text{and Continuous} \\ \text{Liquid} \\ \tau''''_{i_{lv_k}} A_k \end{array} \right] + \left[\begin{array}{l} \text{Interfacial Drag} \\ \text{Between Vapor} \\ \text{and Drops} \\ \tau''''_{i_{ev_k}} A_k \end{array} \right] \\
& + \left[\begin{array}{l} \text{Transverse Momentum} \\ \text{Exchange Due to Mass} \\ \text{Transfer Between Fields} \\ rV + sV \end{array} \right] + \left[\begin{array}{l} \text{Transverse Momentum} \\ \text{Source Term} \\ S_m \end{array} \right] + \left[\begin{array}{l} \text{Viscous and Turbulent} \\ \text{Shear Stress} \\ \nabla \cdot [\alpha_k (\underline{\underline{g}}_k + \underline{\underline{T}}_k^T)] \end{array} \right]
\end{aligned}$$

As in the vertical momentum equations, the pressures in the pressure force term and the velocities in the wall and interfacial drag term are the new time values while all other terms and variables are computed using old time values. The rate of momentum efflux by transverse convection is given as

the sum of the momentum entering (or leaving) the cell through all transverse connections. Momentum convected by transverse velocities (that are in the direction of the transverse velocity being solved for) is the sum of the momentum entering (or leaving) through mesh cell faces connected to the face of the mesh cell for which the momentum equation is being solved. NKII is the number of mesh cells facing the upstream face of the mesh cell and NKJJ is the number facing the downstream face of the mesh cell. Momentum convected out the sides of the mesh cell by velocities that are orthogonal to the velocity to be solved for, but lie in the same horizontal plane, is given by the sum of the momentum convected into (or out of) cells connected to the sides of the transverse momentum mesh cell. The number of cells connected to the mesh cell under consideration, whose velocities are orthogonal to its velocity, is given by NG. The momentum convected through the top and bottom of the mesh cell by vertical velocities is the sum of the momentum convected into (or out of) cells connected to the top and bottom of the mesh cell and depends on the number of cells connected to the top (NCA) and bottom (NCB) of the mesh cell.

A simple linear average is used to obtain velocities at mesh cell faces

$$V_{L_{II}} = \frac{V_{J_{II}} + V_J}{2} \quad (2.18)$$

Linear averages also are used to obtain other variables at a location where they are not defined. Velocities are obtained from the flows computed by transverse momentum equations by dividing the flows by the momentum cell macroscopic density and transverse momentum flow area

$$V_{k_J} = \frac{(\alpha_k \rho_k V_k S \Delta X)_J}{(\alpha_k \rho_k S \Delta X)_J} \quad (2.19)$$

Donor cell differencing is used for all convective terms and the donor phase momentum is convected in the mass transfer terms. The viscous and turbulent shear stresses are discussed in the next section.

3.0 SOURCE, VISCOUS, AND TURBULENCE TERMS

Terms not fully expanded in the presentation of the finite-difference equations in Section 2 are presented in this section. These include the mass, energy and momentum source terms; the viscous shear stress tensors; the turbulent shear stress tensors; the fluid conduction vector; and the turbulent heat flux vector.

3.1 MASS, ENERGY, AND MOMENTUM SOURCE TERMS

Two types of source terms are required for the mass, energy and momentum finite-difference equations. The first type is associated with one-dimensional component connections to the vessel mesh and the second type is associated with arbitrary boundary conditions that may be specified anywhere in the vessel mesh.

3.1.1 Vessel Connection Source Terms

The vessel connection energy and mass source terms have an implicit and an explicit term arising from the five-equation drift flux model used in the one-dimensional components. The mixture velocity in the source terms is taken at the new time and represents the implicit portion of the source term. The donor cell quantities (denoted by the * superscript) and the relative velocity are computed using currently known values and are therefore explicit. The donor cell is determined by the sign of the mixture and relative velocities, respectively. If flow is leaving the vessel, then vessel properties are used. If flow is entering the vessel, then properties in the one-dimensional component are used. The finite-difference form of the source terms is as follows:

Vapor Mass Source Term

$$S_{cv} = (\alpha_v \rho_v)^* V_m^n FA + [\alpha_v (1 - \alpha_v) \frac{\rho_l \rho_v}{\rho_m}]^* V_r FA \quad (3.1)$$

Liquid Mass Source Term

$$S_{cl} = \{[(1-\alpha_v)\rho_l]^* V_{mp}^n FA - [\alpha_v(1-\alpha_v) \frac{\rho_l \rho_v}{\rho_m}]^* V_{rp} FA\} (1-\eta)^* \quad (3.2)$$

Entrained Liquid Mass Source Term

$$S_{ce} = \{[(1-\alpha_v)\rho_l]^* V_{mp}^n FA - [\alpha_v(1-\alpha_v) \frac{\rho_l \rho_v}{\rho_m}]^* V_{rp} FA\} \eta^* \quad (3.3)$$

Vapor Energy Source Term

$$S_{ev} = [\alpha_v(\rho_v e_v + P)]^* V_{mp}^n FA + [\alpha_v(1-\alpha_v) \frac{\rho_l \rho_v}{\rho_m} (e_v + \frac{P}{\rho_v})]^* V_{rp} FA \quad (3.4)$$

Liquid Energy Source Term

$$S_{el} = [(1-\alpha_v)(\rho_l e_l + P)]^* V_{mp}^n FA - [\alpha_v(1-\alpha_v) \frac{\rho_l \rho_v}{\rho_m} (e_l + \frac{P}{\rho_l})]^* V_{rp} FA \quad (3.5)$$

The velocities are calculated at the junction between the vessel and the one-dimensional component using the five-equation drift flux model, hence the subscript p (for pipe). They are based on the flow area at the junction, FA.

The momentum source terms for the vessel connections are somewhat more complex as they depend on the orientation of the pipe connection. Both horizontal and vertical pipes may be connected to the vessel mesh. However, only one pipe connection is allowed per vessel mesh cell. In all cases it has been assumed that the pipe is normal to the face of the vessel mesh cell. The momentum sources are as follows:

Transverse Momentum Convected Out a Vertical Loop

$$S_{mv} = \begin{cases} -(\alpha_v \rho_v V_v)_J V_{vp} FA & \text{if flow is out of vessel } (V_{vp} \text{ positive}) \\ 0 & \text{if flow is into vessel } (V_{vp} \text{ negative}) \end{cases} \quad (3.6)$$

$$S_{m\ell} = \begin{cases} -(\alpha_{\ell} \rho_{\ell} V_{\ell})_J V_{\ell p} FA & V_{\ell p} > 0 \\ 0 & V_{\ell p} < 0 \end{cases} \quad (3.7)$$

$$S_{me} = \begin{cases} -(\alpha_e \rho_e V_e)_J V_{\ell p} FA & V_{\ell p} > 0 \\ 0 & V_{\ell p} < 0 \end{cases} \quad (3.8)$$

Transverse Momentum Convected by a Horizontal Loop

Normal of cell face is orthogonal to the pipe axis:

$$S_{mv} = \begin{cases} -(\alpha_v \rho_v V_v)_J V_{vJ} S_k \Delta x & \text{if flow is out of vessel } (V_{vp} \text{ positive}) \\ 0 & \text{if flow is into vessel } (V_{vp} \text{ negative}) \end{cases} \quad (3.9)$$

$$S_{m\ell} = \begin{cases} -(\alpha_{\ell} \rho_{\ell} V_{\ell})_J V_{\ell J} S_k \Delta x & V_{\ell p} > 0 \\ 0 & V_{\ell p} < 0 \end{cases} \quad (3.10)$$

$$S_{me} = \begin{cases} -(\alpha_e \rho_e V_e)_J V_{eJ} S_k \Delta x & V_{\ell p} > 0 \\ 0 & V_{\ell p} < 0 \end{cases} \quad (3.11)$$

Normal of cell face is parallel to the pipe axis:

$$S_{mv} = (\alpha_v \rho_v V_v)^* \left(\frac{V_{vJ} + V_{vp}}{2} \right) A_{CONV} \quad (3.12)$$

$$S_{m\ell} = (\alpha_{\ell} \rho_{\ell} V_{\ell})^* \left(\frac{V_{\ell j} + V_{\ell p}}{2} \right) A_{\text{CONV}} \quad (3.13)$$

$$S_{me} = (\alpha_e \rho_{\ell} V_e)^* \left(\frac{V_{ej} + V_{\ell p}}{2} \right) A_{\text{CONV}} \quad (3.14)$$

In the latter case, the donor cell quantity $(\alpha \rho V)^*$ is computed using pipe variables if the flow is into the vessel or vessel variables if flow is out of the vessel. The area A_{CONV} through which momentum is convected is the minimum of the pipe flow area, FA , and the area of the vessel mesh cell face $S_k \Delta x$. The same logic holds for the following source term.

Vertical Momentum Convected by a Vertical Loop

$$S_{mv} = (\alpha_v \rho_v U_v)^* \left(\frac{U_{vj} + V_{vp}}{2} \right) A_{\text{CONV}} \quad (3.15)$$

$$S_{m\ell} = (\alpha_{\ell} \rho_{\ell} U_{\ell})^* \left(\frac{U_{\ell j} + V_{\ell p}}{2} \right) A_{\text{CONV}} \quad (3.16)$$

$$S_{me} = (\alpha_e \rho_{\ell} U_e)^* \left(\frac{U_{ej} + V_{\ell p}}{2} \right) A_{\text{CONV}} \quad (3.17)$$

Vertical Momentum Convected by a Horizontal Loop

$$S_{mv} = \begin{cases} (\alpha_v \rho_v U_v)_j U_{vj} A_m & V_{vp} > 0 \\ 0 & V_{vp} < 0 \end{cases} \quad (3.18)$$

$$S_{m\ell} = \begin{cases} (\alpha_{\ell} \rho_{\ell} U_{\ell})_j U_{\ell_j} A_m & V_{\ell_p} > 0 \\ 0 & V_{\ell_p} < 0 \end{cases} \quad (3.19)$$

$$S_{me} = \begin{cases} (\alpha_e \rho_e U_e)_j U_{e_j} A_m & V_{\ell_p} > 0 \\ 0 & V_{\ell_p} < 0 \end{cases} \quad (3.20)$$

The pipe velocities are computed from the mixture and relative velocities used in the five-equation drift flux model as follows:

$$V_{\ell_p} = V_m - \frac{\alpha \rho_g}{\rho_m} V_r \quad (3.21)$$

$$V_{v_p} = V_m + \frac{(1-\alpha) \rho_{\ell}}{\rho_m} V_r \quad (3.22)$$

The pipe velocity for the entrained liquid phase is always assumed equal to the liquid velocity in the pipe since only two velocity fields (vapor and liquid) are available in the one-dimensional components.

3.1.2 Boundary Condition Source Terms

There are five basic types of boundary conditions that may be specified within the vessel mesh. The first type allows the user to specify the pressure and the mixture enthalpy in any cell. The normal momentum equations are then solved on the cell faces to obtain flows into or out of the cell. Properties specified within the cell are convected to surrounding cells if the flow is out of the cell. Properties of surrounding cells are convected into the specified cell if the flow is into the cell. However, since the properties of the cell are specified, the pressure, temperature, and void fractions do not change accordingly, so the pressure boundary condition can act as a mass, energy and momentum sink, if flow is into the cell, or source, if flow is out of the cell.

The second type of boundary condition allows the user to specify the mixture enthalpy, and pressure within the cell and the continuity mass flow rate at the top of the cell. It is assumed that all three phases have the same velocity at the cell face. No momentum solution is performed at the top of the cell for this case since the flow is specified. Otherwise, the boundary condition behaves in the same way as the first type of boundary condition, acting as a source (or sink) of mass, momentum, and energy, depending on the direction of flow.

The third type of boundary condition sets the flow on any mesh cell face, and therefore does not produce any mass, momentum, or energy sources.

The fourth type of boundary condition allows the user to specify a mass and energy source in any computational cell without changing the computed fluid properties within the cell. Again, all three phases are assumed to travel at the mixture velocity and the amount of flow is determined by the volume fraction of each phase specified in the boundary condition. Momentum of this source is added only if the flow is in the transverse direction and into the vessel mesh, or if flow is out of mesh.

The final type of boundary condition allows the user to specify a pressure sink to be connected to any cell. A simple momentum equation is solved between the sink pressure and the cell pressure, and the resulting flow produces a mass, momentum, and energy sink if flow is out of the vessel and a mass and energy source if the flow is into the vessel. The sink vapor momentum equation is as follows:

$$\begin{aligned}
 (\alpha_v \rho_v V_v A)_{\text{SINK}}^n &= (\alpha_v \rho_v V_v A)_{\text{SINK}} + \frac{\Delta t}{\Delta x} A_{\text{SINK}} (P_{\text{SINK}} - P_J) \\
 - K_{V_{\text{SINK}}} U_{V_{\text{SINK}}}^n &- k_{v\ell} (U_v - U_\ell)_{\text{SINK}}^n - k_{ve} (U_v - U_e)_{\text{SINK}}^n
 \end{aligned} \tag{3.23}$$

Transverse and vertical momentum is convected out of the vessel mesh by the sink velocity computed from the above equation in the same way that

vessel/pipe connections convect momentum from the mesh, and the same equations may be used to represent the sink momentum sources if the pipe velocity is replaced with the sink velocity in the source equations.

3.2 VISCOUS AND TURBULENT SHEAR STRESS TENSORS AND HEAT FLUX VECTORS

The viscous and turbulent shear stress tensors represented in the finite-difference equation given in Section 2 by τ_{kj}^T are expanded in this section. This term represents the viscous and turbulent stress tensors, $\nabla \cdot [\alpha_k(\underline{\sigma}_k + \underline{\tau}_k^T)]$, of the partial differential equations. The viscous stress tensor may be written as

$$\underline{\sigma}_k = \begin{pmatrix} \sigma_{k_{xx}} & \sigma_{k_{xy}} & \sigma_{k_{xz}} \\ \sigma_{k_{yx}} & \sigma_{k_{yy}} & \sigma_{k_{yz}} \\ \sigma_{k_{zx}} & \sigma_{k_{zy}} & \sigma_{k_{zz}} \end{pmatrix} \quad (3.24)$$

The turbulent stress tensor $\underline{\tau}_k^T$ may be written in a similar way. Further,

$$\begin{aligned} \nabla \cdot [\alpha_k (\underline{\sigma}_k + \underline{\tau}_k^T)] &= \left\{ \frac{\partial}{\partial x} [(\sigma_{k_{xx}} + \tau_{k_{xx}}^T)] + \frac{\partial}{\partial y} [\alpha_k (\sigma_{k_{yx}} + \tau_{k_{yx}}^T)] \right. \\ &+ \frac{\partial}{\partial z} [\alpha_k (\sigma_{k_{zx}} + \tau_{k_{zx}}^T)] \Big\} \underline{i} + \left\{ \frac{\partial}{\partial x} [\alpha_k (\sigma_{k_{xy}} + \tau_{k_{xy}}^T)] \right. \\ &+ \frac{\partial}{\partial y} [\alpha_k (\sigma_{k_{yy}} + \tau_{k_{yy}}^T)] + \frac{\partial}{\partial z} [\alpha_k (\sigma_{k_{zy}} + \tau_{k_{zy}}^T)] \Big\} \underline{j} \\ &+ \left\{ \frac{\partial}{\partial x} [\alpha_k (\sigma_{k_{xz}} + \tau_{k_{xz}}^T)] + \frac{\partial}{\partial y} [\alpha_k (\sigma_{k_{yz}} + \tau_{k_{yz}}^T)] + \frac{\partial}{\partial z} [\alpha_k (\sigma_{k_{zz}} + \tau_{k_{zz}}^T)] \right\} \underline{k} \end{aligned}$$

The coordinate system used is shown in Figure 3.1.

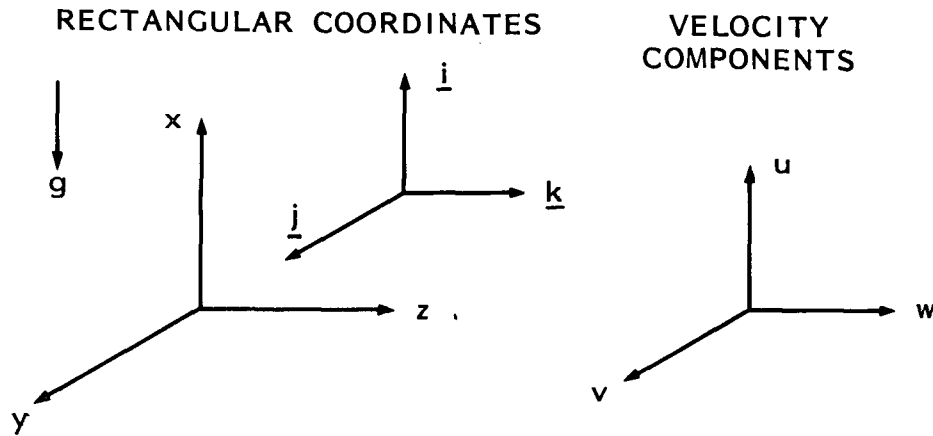


FIGURE 3.1. Coordinate System and Nomenclature

The first subscript on the shear stress denotes the face the stress is acting on and the second subscript the direction the stress acts in. (For example, $\sigma_{k_{ij}}$ is the shear stress acting on face i in the j direction.)

The viscous and turbulent stresses are defined in terms of the bulk deformation tensor, D_{k_B} , given by

$$D_{k_B} = \frac{1}{2} [\nabla \underline{u} + (\nabla \underline{u})^t] \quad (3.26)$$

or

$$D_{k_B} = \begin{pmatrix} \frac{\partial u}{\partial x} & \frac{1}{2} \left(\frac{\partial u}{\partial y} + \frac{\partial v}{\partial x} \right) & \frac{1}{2} \left(\frac{\partial u}{\partial z} + \frac{\partial w}{\partial x} \right) \\ \frac{1}{2} \left(\frac{\partial u}{\partial y} + \frac{\partial v}{\partial x} \right) & \frac{\partial v}{\partial y} & \frac{1}{2} \left(\frac{\partial v}{\partial z} + \frac{\partial w}{\partial y} \right) \\ \frac{1}{2} \left(\frac{\partial u}{\partial z} + \frac{\partial w}{\partial x} \right) & \frac{1}{2} \left(\frac{\partial v}{\partial z} + \frac{\partial w}{\partial y} \right) & \frac{\partial w}{\partial z} \end{pmatrix} \quad (3.27)$$

Eliminating the normal stresses such that the diagonal term is zero gives the deleted bulk deformation tensor $D_{k_B}^*$.

Neglecting the viscous contribution to the normal stresses and eliminating the normal stress due to pressure already accounted for in the finite-difference equation leaves

$$\underline{\underline{\sigma}}_k = 2\mu \underline{\underline{D}}_k^* \quad (3.28)$$

thus,

$$\sigma_{k_{xy}} = \sigma_{k_{yx}} = \mu \left(\frac{\partial u}{\partial y} + \frac{\partial v}{\partial x} \right) \quad (3.29)$$

$$\sigma_{k_{xz}} = \sigma_{k_{zx}} = \mu \left(\frac{\partial u}{\partial z} + \frac{\partial w}{\partial x} \right) \quad (3.30)$$

$$\sigma_{k_{yz}} = \sigma_{k_{zy}} = \mu \left(\frac{\partial v}{\partial z} + \frac{\partial w}{\partial y} \right) \quad (3.31)$$

The turbulent stress tensor is given by

$$\underline{\underline{T}}_k^T = -p_k^T \underline{\underline{F}}_k + 2 \mu_k^T \underline{\underline{D}}_k^* \quad (3.32)$$

p_k^T is the turbulent pressure. $\underline{\underline{F}}$ is the anisotropy tensor which is assumed to be equal to the unit tensor in general. μ_k^T is the turbulent or "eddy" viscosity. The above tensor, $\underline{\underline{T}}_k^T$, may be written in matrix form as

$$\underline{\underline{T}}_k^T = \begin{pmatrix} -P_k^T F_{k_{xx}} & \mu_k^T \left(\frac{\partial u}{\partial y} + \frac{\partial v}{\partial x} \right) & \mu_k^T \left(\frac{\partial u}{\partial z} + \frac{\partial w}{\partial x} \right) \\ \mu_k^T \left(\frac{\partial u}{\partial y} + \frac{\partial v}{\partial x} \right) & -P_k^T F_{k_{yy}} & \mu_k^T \left(\frac{\partial v}{\partial z} + \frac{\partial w}{\partial y} \right) \\ \mu_k^T \left(\frac{\partial u}{\partial z} + \frac{\partial w}{\partial x} \right) & \mu_k^T \left(\frac{\partial v}{\partial z} + \frac{\partial w}{\partial y} \right) & -P_k^T F_{k_{zz}} \end{pmatrix} \quad (3.33)$$

The turbulent viscosity is given by

$$\mu_k^T = \rho_k \ell_m^2 \sqrt{2 D_{k_B}^* : D_{k_B}^*} \quad (3.34)$$

and the turbulent pressure by

$$P_k^T = \rho_k \ell_m^2 (2 D_{k_B}^* : D_{k_B}^*) \quad (3.35)$$

The double dot product of two second order tensors $\underline{\underline{A}}$ and $\underline{\underline{B}}$ is defined as

$$\underline{\underline{A}} : \underline{\underline{B}} = A_{ij} B_{ji} \quad (3.36)$$

In this case this gives

$$2 D_{k_B}^* : D_{k_B}^* = \left(\frac{\partial u}{\partial y} + \frac{\partial v}{\partial x} \right)^2 + \left(\frac{\partial u}{\partial z} + \frac{\partial w}{\partial x} \right)^2 + \left(\frac{\partial v}{\partial z} + \frac{\partial w}{\partial y} \right)^2 \quad (3.37)$$

Now that all of the terms for the viscous and turbulent shear stresses have been expanded, the finite-difference form of the terms can be presented. The total force resulting from viscous and turbulent shear stresses acting on a mesh cell may be obtained using the divergence theorem:

$$\underline{F} = \iiint_{vol} \nabla \cdot [\alpha_k (\underline{\sigma}_k + \underline{T}_k^T)] dx = \iint_{surface} \underline{n} \cdot [\alpha_k (\underline{\sigma}_k + \underline{T}_k^T)] ds \quad (3.38)$$

The finite-difference approximation for this total force is

$$\begin{aligned} \underline{F} = & \underline{i} \cdot \{ \alpha_k (\sigma_{k_{xx}} + T_{k_{xx}}^T) |_{+x} \Delta y \Delta z - \alpha_k (\sigma_{k_{xx}} + T_{k_{xx}}^T) |_{-x} \Delta y \Delta z \\ & + \alpha_k (\sigma_{k_{yx}} + T_{k_{yx}}^T) |_{+y} \Delta x \Delta z - \alpha_k (\sigma_{k_{yx}} + T_{k_{yx}}^T) |_{-y} \Delta x \Delta z \\ & + \alpha_k (\sigma_{k_{zx}} + T_{k_{zx}}^T) |_{+z} \Delta x \Delta y - \alpha_k (\sigma_{k_{zx}} + T_{k_{zx}}^T) |_{-z} \Delta x \Delta y \} \\ & + \underline{j} \cdot \{ \alpha_k (\sigma_{k_{xy}} + T_{k_{xy}}^T) |_{+x} \Delta y \Delta z - \alpha_k (\sigma_{k_{xy}} + T_{k_{xy}}^T) |_{-x} \Delta y \Delta z \\ & + \alpha_k (\sigma_{k_{yy}} + T_{k_{yy}}^T) |_{+y} \Delta x \Delta z - \alpha_k (\sigma_{k_{yy}} + T_{k_{yy}}^T) |_{-y} \Delta x \Delta z \\ & + \alpha_k (\sigma_{k_{zy}} + T_{k_{zy}}^T) |_{+z} \Delta x \Delta y - \alpha_k (\sigma_{k_{zy}} + T_{k_{zy}}^T) |_{-z} \Delta x \Delta y \} \\ & + \underline{k} \cdot \{ \alpha_k (\sigma_{k_{xz}} + T_{k_{xz}}^T) |_{+x} \Delta y \Delta z - \alpha_k (\sigma_{k_{xz}} + T_{k_{xz}}^T) |_{-x} \Delta y \Delta z \\ & + \alpha_k (\sigma_{k_{yz}} + T_{k_{yz}}^T) |_{+y} \Delta x \Delta z - \alpha_k (\sigma_{k_{yz}} + T_{k_{yz}}^T) |_{-y} \Delta x \Delta z \end{aligned}$$

$$+ \alpha_k (\sigma_{k_{zz}} + T_{k_{zz}}^T) |_{+z} \Delta x \Delta y - \alpha_k (\sigma_{k_{zz}} + T_{k_{zz}}^T) |_{-z} \Delta x \Delta y \quad (3.39)$$

The various stresses ($\sigma_{k_{xx}}$, $T_{k_{xx}}^T$, $\sigma_{k_{yx}}$, $T_{k_{yx}}^T$, etc.) must be evaluated on various surfaces of vertical and transverse momentum cells. For example, the stresses acting in the vertical direction on a vertical momentum cell are shown in Figure 3.2.

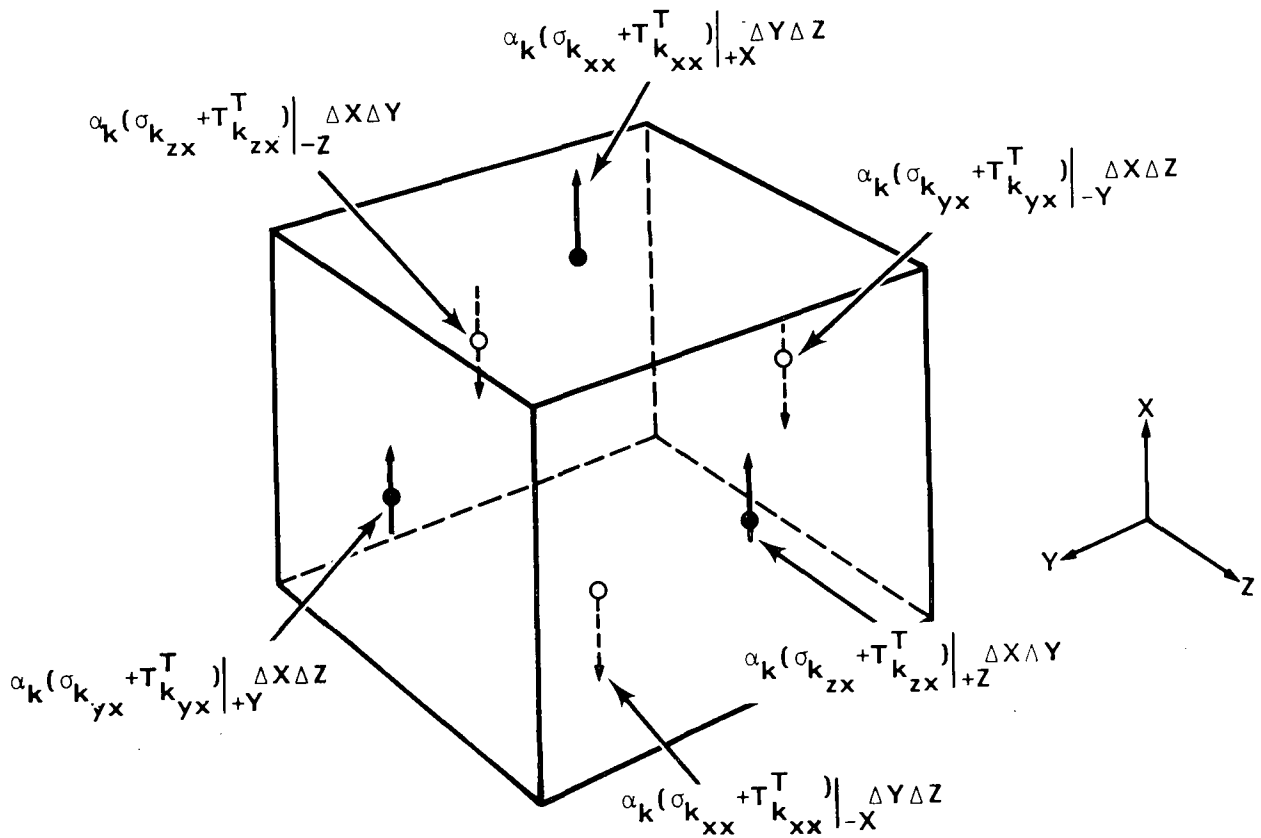


FIGURE 3.2. Vertical Stresses Acting on Vertical Momentum Cell

The velocity gradients are calculated by taking differences between adjacent cell velocities to obtain values for $\Delta u/\Delta z$ and $\Delta w/\Delta \ell$ on continuity cell edges. This is illustrated in Figure 3.3.

In this figure, the velocity gradient at point A is given by:

$$\left(\frac{\partial u}{\partial z} + \frac{\partial w}{\partial x}\right)_A = \left(\frac{u_2 - u_1}{\Delta \ell} + \frac{w_2 - w_1}{\Delta x}\right) \quad (3.40)$$

The derivatives for the other edges (B, C, D, E, F, G, H, I, J, K, L) are computed in a similar fashion and the process is repeated for other cells. If a solid surface bounds the cell in the transverse direction, it is assumed that the velocity gradient is zero at the wall. Velocity is assumed to be zero at the wall for solid surfaces that bound the cell in a vertical direction.

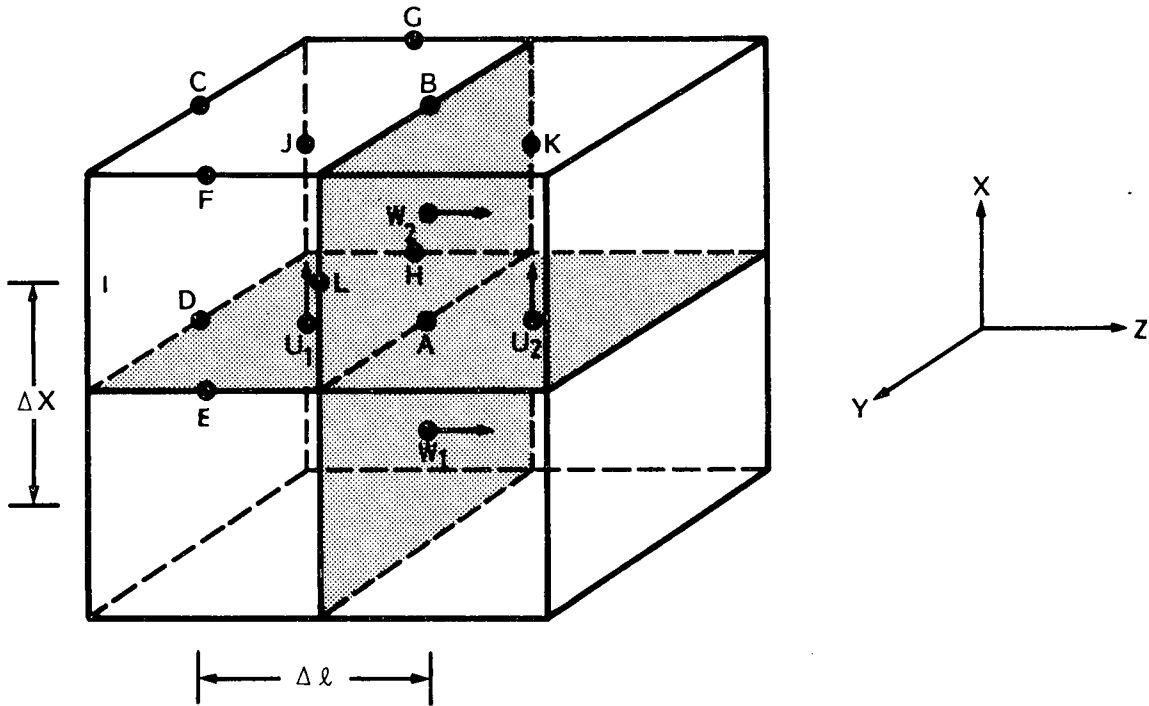


FIGURE 3.3. Velocity Gradient for Point A

The derivative at the mass cell center is obtained by taking a four-point average of the derivatives on the cell edges:

$$\begin{aligned} \left(\frac{\partial u}{\partial z} + \frac{\partial w}{\partial x} \right)_{\text{cell center}} = \frac{1}{4} \{ & \left(\frac{\partial u}{\partial z} + \frac{\partial w}{\partial x} \right)_A + \left(\frac{\partial u}{\partial z} + \frac{\partial w}{\partial x} \right)_B \\ & + \left(\frac{\partial u}{\partial z} + \frac{\partial w}{\partial x} \right)_C + \left(\frac{\partial u}{\partial z} + \frac{\partial w}{\partial x} \right)_D \} \end{aligned} \quad (3.41)$$

The same procedure is used to find $\left(\frac{\partial u}{\partial y} + \frac{\partial v}{\partial x} \right)$ and $\left(\frac{\partial v}{\partial z} + \frac{\partial w}{\partial x} \right)$ at the mass cell center. The quantity $2\underline{D}_{k_B}^* : \underline{D}_{k_B}^*$ at the cell center is then calculated from Equation 3.37 using these averaged derivatives. The turbulent viscosity and turbulent pressure are then calculated at the cell center using Equations 3.34 and 3.35.

The shear stress acting on the sides of the momentum cell is computed from the appropriate velocity gradients calculated on that face and the fluid properties at these locations are computed using a four-point average of the properties in the surrounding four mass cells.

The turbulent thermal diffusivity for the mass cell center is computed from the double dot product of the deformation tensor in the same manner as the turbulent viscosity was obtained using the expression:

$$\epsilon_k^T = \ell_h \ell_m \sqrt{2\underline{D}_{k_B}^* : \underline{D}_{k_B}^*} \quad (3.42)$$

The sum of the conduction and turbulent heat flux between two mass cells is then computed from

$$(q_{k_J} + q_{k_J}^T)|_{+x} = - \rho_k (\epsilon_k + \epsilon_k^T) \frac{(h_{J+1} - h_{J-1})}{\Delta x_J} \quad (3.43)$$

The heat fluxes from all surrounding cells are summed up to give the net heat flux into cell J.

Since the viscous and turbulent shear stresses are computed explicitly, the time step is limited by the criterion

$$\Delta t < \min \left[\frac{1}{\frac{2(\mu + \mu^T)}{\rho \Delta x^2} + \frac{u}{\Delta x}} \right]_j$$

4.0 NUMERICAL SOLUTION

The equations shown in Sections 2 and 3 form a set of algebraic equations that must be solved simultaneously to obtain a solution for the flow fields involved. These equations must be simultaneously satisfied not only for each cell but for the entire computational mesh. The numerical scheme chosen to solve these equations must be as efficient as possible in order to obtain a solution in a reasonable amount of computer time. While the equations can be solved directly using Gaussian elimination, the computer time required for problems with many mesh cells would be prohibitive. Therefore, it is desirable to reduce the number and complexity of the equations being solved as much as possible and use the most efficient scheme possible to obtain a final solution. Note that the equations in Sections 2 and 3 have already been greatly simplified over the conservation equations they are intended to represent since they are written in a semi-implicit form. It is assumed that these semi-implicit equations converge to the correct solution if a time step size smaller than that required by the Courant criterion is used. The methods used to solve these equations will now be described.

4.1 SOLUTION OF THE MOMENTUM EQUATIONS

The momentum equations are solved first in the solution procedure using currently known values for all of the variables, to obtain an estimate of the new time flow. All explicit terms and variables in the momentum equation are computed in this step and are assumed to remain constant during the remainder of the time step. The semi-implicit momentum equations (Equations 2.8 - 2.10 and 2.15 - 2.17) have the form:

Liquid

$$F_L = A_1 + B_1 \Delta P + C_1 F_L + D_1 F_V \quad (4.1)$$

Vapor

$$F_V = A_2 + B_2 \Delta P + C_2 F_L + D_2 F_V + E_2 F_E \quad (4.2)$$

Entrained Liquid

$$F_E = A_3 + B_3 \Delta P + D_3 F_V + E_3 F_E \quad (4.3)$$

A_1 , A_2 , and A_3 are constants that represent the explicit terms in the momentum equations such as the momentum efflux terms and the gravitational force. B_1 , B_2 , and B_3 are the explicit portion of the pressure gradient force term, C_1 , and C_2 are the explicit factors that multiply the liquid flow rate in the wall and interfacial drag terms. D_1 , D_2 , D_3 , E_2 , and E_3 are the corresponding terms that multiply the vapor and entrained liquid flow rates. F_L is the liquid mass flow rate, F_V is the vapor mass flow rate, and F_E is the entrained liquid mass flow rate. These equations may be written in matrix form as

$$\begin{bmatrix} C_1^{-1} & D_1 & 0 \\ C_2 & D_2^{-1} & E_2 \\ 0 & D_3 & E_3^{-1} \end{bmatrix} \begin{Bmatrix} F_L \\ F_V \\ F_E \end{Bmatrix} = \begin{Bmatrix} -A_1 - B_1 \Delta P \\ -A_2 - B_2 \Delta P \\ -A_3 - B_3 \Delta P \end{Bmatrix} \quad (4.4)$$

Equation 4.4 is solved by Gaussian elimination to obtain a solution for the phasic mass flow rates as a function of the pressure gradient across the momentum cell, ΔP :

$$F_L = G_1 + H_1 \Delta P$$

$$F_V = G_2 + H_2 \Delta P$$

$$F_E = G_3 + H_3 \Delta P \quad (4.5)$$

The mass flow rates given by Equation 4.5 are computed based on the mass of each phase contained within the momentum control volume. Velocities may be computed from these flow rates using Equation 2.14. Once the tentative velocities have been obtained from the momentum equations the continuity and energy equations can be solved.

4.2 LINEARIZATION OF THE MASS AND ENERGY EQUATIONS

If the right hand side of each of the mass and energy equations is moved to the left hand side, the sum of the terms on the left side should be identically equal to zero if the current values of all variables satisfy the equations. The energy and mass equations will not generally be satisfied when the new velocities computed from the momentum equations are used to compute the convective terms in these equations. There will be some residual error in each equation as a result of the new velocities and changes in the magnitude of some of the explicit terms in the mass and energy equations such as the vapor generation rate. The vapor mass equation, for example, has a residual error given by

$$\begin{aligned} & \frac{[(\alpha_V \rho_V)_J^n - (\alpha_V \rho_V)_J] A_{CJ}}{\Delta t} + \sum_{KA=1}^{NA} \frac{[(\alpha_V \rho_V)^* \tilde{U}_{Vj} A_j]_{KA}}{\Delta x_J} \\ & - \sum_{KB=1}^{NB} \frac{[(\alpha_V \rho_V)^* \tilde{U}_{Vj-1} A_{j-1}]_{KB}}{\Delta x_J} - \sum_{L=1}^{NKK} S_L [(\alpha_V \rho_V)^* \tilde{V}_{VL}]_J \end{aligned}$$

$$-\frac{r_J}{\Delta x_J} - \frac{S_{cvJ}}{\Delta x_J} = E_{CV} \quad (4.6)$$

All terms are computed using currently known values for each of the variables. The \sim symbol over the velocities indicates that they are the tentative values computed from the momentum equations (Equation 4.5). The mass equations for the liquid phases and the two energy equations also have residual errors: E_{CL} , E_{CE} , E_{EV} , and E_{EL} . The equations are simultaneously satisfied when E_{CV} , E_{CL} , E_{CE} , E_{EV} , and E_{EL} for all cells in the mesh simultaneously approach zero. The variation of each of the independent variables required to bring the residual errors to zero can be obtained using the block Newton-Raphson method (Ref. 2). This is done by linearizing the equations with respect to the independent variables P , α_v , $\alpha_v h_v$, $(1-\alpha_v)h_\ell$, and α_e to obtain the following equation for each cell.

$$\begin{bmatrix} \frac{\partial E_{CL}}{\partial \alpha_v} & \frac{\partial E_{CL}}{\partial \alpha_v h_v} & \frac{\partial E_{CL}}{\partial (1-\alpha_v) h_\ell} & \frac{\partial E_{CL}}{\partial \alpha_e} & \frac{\partial E_{CL}}{\partial P_J} & \frac{\partial E_{CL}}{\partial P_{i=1}} & \cdots & \frac{\partial E_{CL}}{\partial P_{i=NCON}} \\ \frac{\partial E_{EV}}{\partial \alpha_v} & \frac{\partial E_{EV}}{\partial \alpha_v h_v} & \frac{\partial E_{EV}}{\partial (1-\alpha_v) h_\ell} & \frac{\partial E_{EV}}{\partial \alpha_e} & \frac{\partial E_{EV}}{\partial P_J} & \frac{\partial E_{EV}}{\partial P_{i=1}} & \cdots & \frac{\partial E_{EV}}{\partial P_{i=NCON}} \\ \frac{\partial E_{EL}}{\partial \alpha_v} & \frac{\partial E_{EL}}{\partial \alpha_v h_v} & \frac{\partial E_{EL}}{\partial (1-\alpha_v) h_\ell} & \frac{\partial E_{EL}}{\partial \alpha_e} & \frac{\partial E_{EL}}{\partial P_J} & \frac{\partial E_{EL}}{\partial P_{i=1}} & \cdots & \frac{\partial E_{EL}}{\partial P_{i=NCON}} \\ \frac{\partial E_{CE}}{\partial \alpha_v} & \frac{\partial E_{CE}}{\partial \alpha_v h_v} & \frac{\partial E_{CE}}{\partial (1-\alpha_v) h_\ell} & \frac{\partial E_{CE}}{\partial \alpha_e} & \frac{\partial E_{CE}}{\partial P_J} & \frac{\partial E_{CE}}{\partial P_{i=1}} & \cdots & \frac{\partial E_{CE}}{\partial P_{i=NCON}} \\ \frac{\partial E_{CV}}{\partial \alpha_v} & \frac{\partial E_{CV}}{\partial \alpha_v h_v} & \frac{\partial E_{CV}}{\partial (1-\alpha_v) h_\ell} & \frac{\partial E_{CV}}{\partial \alpha_e} & \frac{\partial E_{CV}}{\partial P_J} & \frac{\partial E_{CV}}{\partial P_{i=1}} & \cdots & \frac{\partial E_{CV}}{\partial P_{i=NCON}} \end{bmatrix} \begin{Bmatrix} \delta \alpha_v \\ \delta \alpha_v h_v \\ \delta (1-\alpha_v) h_\ell \\ \delta \alpha_e \\ \delta P_J \\ \delta P_{i=1} \\ \vdots \\ \delta P_{i=NCON} \end{Bmatrix} = - \begin{Bmatrix} E_{CL} \\ E_{EV} \\ E_{EL} \\ E_{CE} \\ E_{CV} \end{Bmatrix}$$

This equation has the form:

$$[R(X)]\{\delta(x)\} = -E \quad (4.7)$$

for each cell. $\text{Det } [R(X)]$ is the Jacobian of the system of equations evaluated for the set of independent variables given by the vector X , δ is the solution vector containing the linear variation of the independent variables, and $-E$ is a vector containing the negative of the residual errors required to bring the error for each equation to zero. The matrix $R(X)$ is composed of analytical derivatives of each of the terms in the equations with respect to the independent variables. The velocities are linearly dependent on the pressures so derivatives of velocities with respect to pressure may be obtained directly from the momentum equations, Equation 4.5. The linear variation of velocity with respect to pressure is given by:

$$\begin{aligned} \delta V_L &= H_1 (\delta P_J - \delta P_{J+1}) \\ \delta V_V &= H_2 (\delta P_J - \delta P_{J+1}) \\ \delta V_E &= H_3 (\delta P_J - \delta P_{J+1}) \end{aligned} \quad (4.8)$$

The derivatives of the other dependent variables such as ρ_ℓ , ρ_v , h_ℓ , and h_v are obtained from the thermal equations of state

$$\begin{aligned} \rho_\ell &= \rho_\ell (P, h_\ell) \\ \rho_v &= \rho_v (P, h_v) \end{aligned} \quad (4.9)$$

and from fundamental identities involving partial derivatives. For example, the derivative of ρ_v with respect to the independent variable $\alpha_v h_v$ is given by

$$\frac{\partial \rho_v}{\partial \alpha_v h_v} = \frac{\partial \rho_v}{\partial h_v} \frac{\partial h_v}{\partial \alpha_v h_v} \quad (4.10)$$

The derivative $\partial \rho_v / \partial h_v$ is obtained directly from the thermal equation of state, while the derivative $\partial h_v / \partial \alpha_v h_v$ is obtained from the identity

$$h_v = \frac{\alpha_v h_v}{\alpha_v} \quad (4.11)$$

The term in the numerator is the independent variable with respect to which the derivative is being taken and the denominator is the independent variable α_v which is assumed to be held constant while taking the derivative. From Equation 4.11 we then obtain

$$\frac{\partial h_v}{\partial \alpha_v h_v} = \frac{1}{\alpha_v} \quad \text{in the extremity of } \alpha_v \rightarrow 0 \quad (4.12)$$

Derivatives of the independent variables are obtained directly from Equation 4.6 and the comparable equations for the other four residual errors. For example, the derivative of the temporal term of Equation 4.6 with respect to α_v is given by

$$\frac{\partial (\alpha_v \rho_v)}{\partial \alpha_v} = \left(\rho_v \frac{\partial \alpha_v}{\partial \alpha_v} + \alpha_v \frac{\partial \rho_v}{\partial \alpha_v} \right) = \rho_v \quad (4.13)$$

Once all of the derivatives for the five equations have been calculated, Equation 4.7 is reduced using Gaussian elimination to obtain solutions for the independent variables of the form

$$\delta P_J = a_5 + \sum_{i=1}^{NCON} g_{5i} \delta P_i \quad (4.14)$$

and

$$\delta \alpha_e = a_4 + e_4 \delta \alpha_e + f_4 \delta P_J + \sum_{i=1}^{NCON} g_{4i} \delta P_i \quad (4.15)$$

$$\delta[(1-\alpha_v)h_\ell] = a_3 + d_3 \delta[(1-\alpha_v)h_\ell] + e_3 \delta \alpha_e + f_3 \delta P_J + \sum_{i=1}^{NCON} g_{3i} \delta P_i \quad (4.16)$$

$$\delta \alpha_v h_v = a_2 + c_2 \delta \alpha_v h_v + d_2 \delta[(1-\alpha_v)h_\ell] + e_2 \delta \alpha_e + f_2 \delta P_J + \sum_{i=1}^{NCON} g_{2i} \delta P_i \quad (4.17)$$

$$\delta \alpha_v = a_1 + b_1 \delta \alpha_v + c_1 \delta \alpha_v h_v + d_1 \delta[(1-\alpha_v)h_\ell] + e_1 \delta \alpha_e + f_1 \delta P_J + \sum_{i=1}^{NCON} g_{1i} \delta P_i \quad (4.18)$$

The computer time required to solve Equation 4.7 is greatly reduced if the

nonlinear coefficients a_k through g_k are assumed to remain constant during a time step and a solution is obtained only for the linearized system of equations (Equations 4.14 through 4.18). Time step controls are then imposed to assure that the variation of the nonlinear terms between time steps remains within acceptable limits so that a stable solution is obtained. A great savings in computer time is realized when this is done since the matrix equation (Equation 4.7) is reduced only once per time step.

4.3 SOLUTION OF THE SYSTEM PRESSURE MATRIX

The linear variation of the pressure in cell J as a function of surrounding cell pressures is given by Equation 4.14. A similar equation may be derived for each cell in the mesh. This set of equations for the pressure variation in each mesh cell must be simultaneously satisfied. The solution to this equation set may be obtained by direct inversion for problems containing only a few mesh cells or by using a Gauss-Siedel iterative technique for problems containing a large number of mesh cells.

The efficiency of the Gauss-Siedel iteration is increased in two ways. First, a direct inversion is carried out over groups of mesh cells specified by the user. The pressure variation for cells within the group are solved simultaneously while the pressure variations in surrounding mesh cells are assumed to have their last iterate value. A Gauss-Siedel iteration is then carried out over the groups of cells where the pressure variations of bounding cells for each group are updated with their last iterate value. As far as the iterative solution is concerned, solving groups of cells by direct inversion has the effect of reducing a large multidimensional problem down to a simpler one-dimensional problem that has the same number of cells as the large problem has groups of cells. Convergence difficulties that are typical of problems with large aspect ratios (long, narrow cells) are also eliminated by placing cells with large aspect ratios between them within the same solution group. The iteration is assumed to have converged when the change in linear pressure variation between time steps is below a specified limit.

The second method for increasing the efficiency of the iteration involves obtaining the initial estimate for the pressure variation in each cell. This

is done through a process called rebalancing. Rebalancing is simply the process of reducing the multidimensional mesh to a one-dimensional mesh for the vessel and then obtaining a solution for the pressure variation at each level of the one-dimensional problem by direct inversion using the methods described above. The one-dimensional solution for the linear pressure variation at each level is then used as an initial guess for the linear pressure variation in each mesh cell on that level in the multidimensional problem. This process greatly enhances the rate of convergence in many problems since the one-dimensional solution generally gives a good estimate for the magnitude of the linear pressure variation in the multidimensional problem. Rebalancing is optional and must be specified by the user. If this option is not used then the initial guess for the linear pressure variation in each cell is zero.

4.4 UNFOLDING OF INDEPENDENT AND DEPENDENT VARIABLES

Once a solution for the linear pressure variation in each cell has been obtained, the linear variation in the other independent variables is unfolded using Equations 4.15 through 4.18. The new value for each of the independent variables is then updated as follows:

$$\begin{aligned}
 P_J^n &= P_J + \delta P_J \\
 \alpha_V^n &= \alpha_V + \delta \alpha_V \\
 \alpha_e^n &= \alpha_e + \delta \alpha_e \\
 (\alpha_V h_V)^n &= \alpha_V h_V + \delta \alpha_V h_V \\
 [(1 - \alpha_V) h_\ell]^n &= (1 - \alpha_V) h_\ell + \delta (1 - \alpha_V) h_\ell
 \end{aligned}
 \tag{4.19}$$

The new time liquid volume fraction is simply, $\alpha_\ell^n = 1.0 - \alpha_V^n - \alpha_e^n$.

The dependent variables h_V and h_ℓ are calculated as follows:

$$h_V^n = \frac{(\alpha_V h_V)^n}{\alpha_V^n}$$

$$h_L^n = \frac{[(1 - \alpha_V) h_L]^n}{(1 - \alpha_V^n)} \quad (4.20)$$

The new time densities are then obtained from the equations of state

$$\rho_V^n = \rho_V(p^n, h_V^n)$$

$$\rho_L^n = \rho_L(p^n, h_L^n) \quad (4.21)$$

The velocities are then updated by

$$V_k^n = V_k + \delta V_k \quad (4.22)$$

where δV_k is given by Equation 4.8.

4.5 PRESSURE EQUATION FOR CELLS CONNECTED TO ONE-DIMENSIONAL COMPONENTS

The equation for the linear pressure variation in vessel mesh cells that connect to one-dimensional components is slightly more complicated than Equation 4.14 since the cell pressure is dependent on the pressures within the one-dimensional component. If the one-dimensional component forms part or all of a loop connecting to one or more additional cells within the vessel, then the pressure variations within the one-dimensional components are functions of the pressure variation within each vessel mesh cell to which the loop connects. The equations for the one-dimensional components in each loop are reduced in TRAC to the form

$$\delta V_i = A_i + \sum_{J=1}^{NVCONIL} B_J \delta P_{v_J} \quad (4.23)$$

where

$$\delta P_{v_J} = a_5 + \sum_{i=1}^{NCON} g_{5_i} \delta P_i + c_j \delta V_i \quad (4.24)$$

where δP_{v_J} is the linear variation in pressure for the vessel computational cell J, δP_i are the linear variations in pressure for other cells that connect to cell J, and δV_i is the linear variation in the junction velocity connecting a one-dimensional TRAC component to cell J.

Combining Equations 4.23 and 4.24, one obtains

$$\delta P_{v_J} = d_j + \sum_{i=1}^{NCON} e_i \delta P_i + \sum_{k=1}^{NVCONIL} f_k \delta P_k \quad (4.25)$$

for the linear variation in pressure for the vessel computational cell J. The second term on the right hand side accounts for the effect of pressure variations in surrounding cells on the pressure in cell J and the third term accounts for the effect of pressure variations in cells that connect to the same one-dimensional component loop as is connected to cell J. This equation, combined with the remaining linearized equations in the vessel model, provides a closed set of linear equations that may be solved by the methods described above. The junction velocities are obtained from Equation 4.23 after the pressures for each cell in the vessel have been obtained.

4.6 TIME STEP CONTROL

Checks are made on the value of each of the new time variables to assure that the variation of the new time variables from the old falls within

reasonable limits. If the new time variables have nonphysical values (e.g., void fractions less than zero or greater than 1.0) or if the variation of the new time variable from the old is unreasonably large, then the solution is backed up to the beginning of the time step, the variables are set to their old time value, the time step is halved, and the time step is repeated. This is done so that the linearized equations will be sufficiently representative of the nonlinear equations to provide an acceptable level of accuracy in the calculation. The time step size is also controlled by the rate of change of the independent variables for the same reason. The stability of the solution is further enhanced by using logarithmic damping between the old and new time values of some of the explicit terms, in particular the interfacial drag and heat transfer coefficients.

REFERENCES

1. D. R. Liles and others, TRAC-PD2 An Advanced Best-Estimate Computer Program for Pressurized Water Reactor Loss-of-Coolant Accident Analysis, NUREG/CR-2054, April 1981.
2. D. R. Liles and W. H. Reed, 1978. "A Semi-Implicit Method for Two-Phase Fluid Dynamics." J. of Comp. Physics 26, No. 3, 390-407.

DISTRIBUTION

No. of
Copies

No. of
Copies

OFFSITE

ONSITE

335 U.S. Nuclear Regulatory
Commission
Division of Technical
Information and Document
Control
7920 Norfolk Avenue
Bethesda, MD 20014

50 Pacific Northwest Laboratory

MJ Thurgood (43)
Publishing Coordination (2)
Technical Information ED (5)

5 James Han
U.S. Nuclear Regulatory
Commission
7915 Eastern Ave.
M/S 1130-SS
Silver Spring, MD 20910

NRC FORM 335 <small>(11-81)</small>		U.S. NUCLEAR REGULATORY COMMISSION BIBLIOGRAPHIC DATA SHEET		1. REPORT NUMBER (Assigned by DDC) NUREG/CR-3046, Vol. 2 PNL-4385	
4. TITLE AND SUBTITLE (Add Volume No., if appropriate) COBRA/TRAC - A Thermal-Hydraulics Code for Transient Analysis of Nuclear Reactor Vessels and Primary Coolant Systems - Vol. 2: COBRA/TRAC Numerical Solution Methods				2. (Leave blank)	
7. AUTHOR(S) M. J. Thurgood, T. L. George				3. RECIPIENT'S ACCESSION NO.	
9. PERFORMING ORGANIZATION NAME AND MAILING ADDRESS (Include Zip Code) Pacific Northwest Laboratory PO Box 999 Richland, Washington 99352				5. DATE REPORT COMPLETED MONTH YEAR November 1982	
12. SPONSORING ORGANIZATION NAME AND MAILING ADDRESS (Include Zip Code) Division of Accident Evaluation Office of Nuclear Regulatory Research U.S. Nuclear Regulatory Commission Washington, DC 20555				6. (Leave blank)	
10. PROJECT/TASK/WORK UNIT NO.				8. (Leave blank)	
11. FIN NO. FIN B2391				13. TYPE OF REPORT Computer Code Manual	
15. SUPPLEMENTARY NOTES				14. (Leave blank)	
16. ABSTRACT (200 words or less) The COBRA/TRAC computer program has been developed to predict the thermal-hydraulic response of nuclear reactor primary coolant systems to small and large break loss-of-coolant accidents and other anticipated transients. The code solves the compressible three-dimensional, two-fluid, three-field equations for two-phase flow in the reactor vessel. The three fields are the vapor field, the continuous liquid field, and the liquid drop field. A five-equation drift flux model is used to model fluid flow in the primary system piping, pressurizer, pumps, and accumulators. The heat generation rate of the core is specified by input and no reactor kinetics calculations are included in the solution. This volume describes the finite-difference equations and the numerical solution methods used to solve these equations. It is directed toward the user who is interested in gaining a more complete understanding of the numerical methods used to obtain a solution to the hydrodynamic equations.					
17. KEY WORDS AND DOCUMENT ANALYSIS					
17a. DESCRIPTORS					
17b. IDENTIFIERS/OPEN-ENDED TERMS					
18. AVAILABILITY STATEMENT Unlimited				19. SECURITY CLASS (This report) Unclassified	
20. SECURITY CLASS (This page) Unclassified				21. NO. OF PAGES	
22. PRICE \$					

UNITED STATES
NUCLEAR REGULATORY COMMISSION
WASHINGTON, D.C. 20555

OFFICIAL BUSINESS
PENALTY FOR PRIVATE USE, \$300

FOURTH-CLASS MAIL
POSTAGE & FEES PAID
USNRC
WASH. D. C.
PERMIT No. G-67

NUREG/CH-3040, Vol. 2

CORRA/TAC - A THERMAL-HYDRAULICS CODE FOR TRANSIENT ANALYSIS
OF NUCLEAR REACTOR VESSELS AND PRIMARY COOLANT SYSTEMS

MARCH 1983